Final Technical Report

An all-oxide epitaxial SNS Josephson junction process

for Navy Research Laboratory

1. Research Objective

The fundamental goal of this two year program was to

- develop a circuit-compatible S-N-S type junction technology based on YBCO.

2. List of Technical Results on Edge Junctions.

Our efforts to develop epitaxial SNS junctions in the edge geometry have been extensively published during the last couple of years. The list of publication is as follows, and the reprints and preprints are attached as a major part of this final report.

2-1. SNS edge junctions using $CaRuO_3$ and $SrRuO_3$ barriers

[1] "High T_c superconductor-normal-superconductor Josephson junctions using $CaRuO_3$ as the metallic barrier", K. Char, M. S. Colclough, T. H. Geballe, and K. E. Myers, Appl. Phys. Lett. **62**, 196 (1993).

[2] "Josephson coupling of $YBa_2Cu_3O_{7-x}$ through a ferromagnetic barrier $SrRuO_3$", L. Antognazza, K. Char, T. H. Geballe, L. L. H. King, and A. W. Sleight, Appl. Phys. Lett. **63**, 1005 (1993).

2-2. Investigation of interface resistance

[3] "Study of interface resistances in epitaxial $YBa_2Cu_3O_{7-x}$/barrier/ $YBa_2Cu_3O_{7-x}$ junctions", K. Char, L. Antognazza, and T. H. Geballe, Appl. Phys. Lett. **63**, 2420 (1993).

[4] "Noise characteristics of $YBa_2Cu_3O_{7-x}/CaRuO_3/YBa_2Cu_3O_{7-x}$ Josephson junctions", K. E. Myers, K. Char, M. S. Colclough, and T. H. Geballe, Appl. Phys. Lett. **64**, 788 (1994).

2-3. Co-doped YBCO barrier edge junctions

[5] "Properties of $YBa_2Cu_3O_{7-x}/YBa_2Cu_{2.79}Co_{0.21}O_{7-x}/YBa_2Cu_3O_{7-x}$ edge junctions", K. Char, L. Antognazza, and T. H. Geballe, Appl. Phys. Lett. **65**, 904 (1994).

[6] "Proximity effect in $YBa_2Cu_3O_{7-\delta}/YBa_2(Cu_{1-x}Co_x)_3O_{7-\delta}/YBa_2Cu_3O_{7-\delta}$ junctions: from the clean limit to the dirty limit with pair breaking", L. Antognazza, S. J. Berkowitz, T. H. Geballe, and K. Char, Phys. Rev. B **51**, 8560 (1995).

2-4. Ca-doped YBCO barrier edge junctions

[7] "Properties of high T_c Josephson junctions with Ca-doped $YBa_2Cu_3O_{7-\delta}$ as a barrier layer", L. Antognazza, B. H. Moeckly, T. H. Geballe, and K. Char, to be published in Phys. Rev. B.

2-5. TEM investigation on SNS junction microstructures

[8] "Origin of nonuniform properties of $YBa_2Cu_3O_{7-x}/CaRuO_3/YBa_2Cu_3O_{7-x}$ Josephson edge junctions", E. Olsson and K. Char, Appl. Phys. Lett. **64**, 1292 (1994).

[9] "Interface microstructure and composition of $YBa_2Cu_3O_{7-\delta}/N/YBa_2Cu_3O_{7-\delta}$ SNS edge junctions with $CaRuO_3$ as the metallic barrier", S. Rozeveld, K. L. Merkle, and K. Char, submitted to Physica C.

[10] "Interface structure of a $YBa_2Cu_3O_{7-\delta}/N/YBa_2Cu_3O_{7-\delta}$ SNS Josephson junction using $YBa_2Cu_{2.79}Co_{0.21}O_{7-\delta}$ as the normal barrier", S. Rozeveld, K. L. Merkle, and K. Char, submitted to Journal of Material Research.

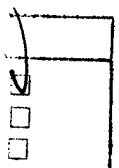

3. C-axis Trilayer SNS Junction Using Co-doped YBCO Barriers

During the last few months, trilayer junctions in the c-axis direction have been laid out, fabricated and tested. The geometry of the junctions is described in Fig. 1. Two separate Au contacts were made to the top YBCO to rule out the effect of contact resistance between the YBCO and Au electrode on the measured junction properties.

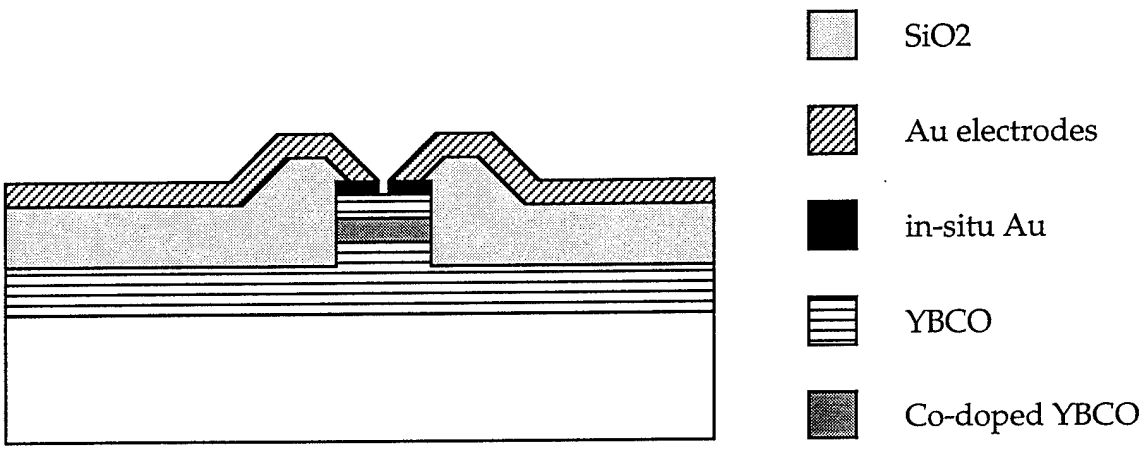

Fig. 1. Schematic cross sectional view of the c-axis trilayer junctions using Co-doped YBCO barrier.

The electrical characteristics of these trilayer junctions varied significantly from junction to junction with nominally the same barriers, suggesting a highly complex mechanism through the barrier. For example, a nice RSJ-like behavior has been observed on a junction with a 160 nm thick barrier of 6.7 % Co-doped YBCO, as shown in Fig. 2. However, some junctions had a well defined resistance but showed no supercurrent, while some of them showed very flux-flow-like IV

characteristics with high I_c. At this point we cannot rule out the possibility of pin-holes in these junctions.

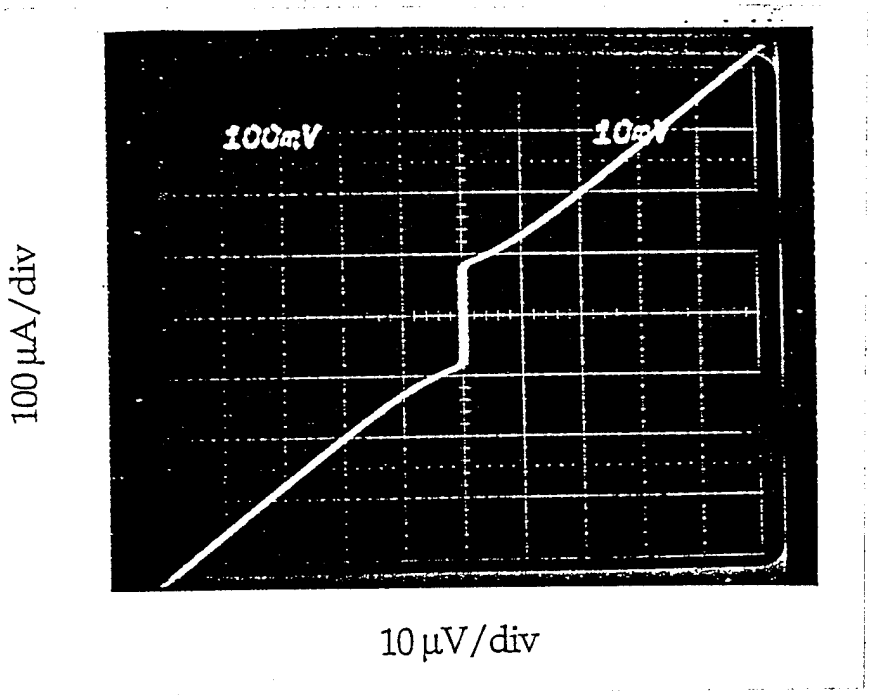

Fig. 2. The I-V characteristic at 53 K of a 20 x 20 μm^2 c-axis trilayer junction made with a 160 nm thick barrier of $YBa_2Cu_{2.8}Co_{0.2}O_{7-\delta}$.

In spite of the large junction area associated with trilayer junction geometry, the high resistivity of the Co-doped YBCO barrier in the c-axis direction may allow us to fabricate a junction of 4 x 4 μm^2 size with a decent resistance. In order to explore the possibility of the c-axis trilayer junctions further, we will need a systematic study of the temperature and barrier thickness dependence of the junction I_c and R_n. However, this work will be out of the scope of this project.

High T_c superconductor-normal-superconductor Josephson junctions using $CaRuO_3$ as the metallic barrier

K. Char, M. S. Colclough, T. H. Geballe,[a] and K. E. Myers[a]
Conductus, Inc., Sunnyvale, California 94086

(Received 19 August 1992; accepted for publication 5 November 1992)

Josephson junctions of the SNS type have been fabricated in the edge and trilayer junction geometries using $YBa_2Cu_3O_{7-\delta}/CaRuO_3/YBa_2Cu_3O_{7-\delta}$. The conducting oxide $CaRuO_3$ was chosen because it grows epitaxially on $YBa_2Cu_3O_{7-\delta}$ and its resistivity shows metallic behavior. Current-voltage characteristics display behavior with significant deviations from the resistivity shunted junction model. The dependence of critical currents and junction resistances on the $CaRuO_3$ thickness suggest that the interface resistance between $YBa_2Cu_3O_{7-\delta}$ and $CaRuO_3$ plays an important role in determining the critical parameters of the junctions. A dc SQUID functioning at 77 K has been demonstrated with this type of junction.

Superconducting-normal-superconducting (SNS) type devices using $YBa_2Cu_3O_7$ (YBCO) have been investigated by several groups studying Josephson junctions. Noble metals such as Au,[1] Ag,[2,3] and then AuAg[3] alloys have been used as the normal material in the microbridge geometry. Trilayer and edge junction geometries require barrier materials which grow epitaxially on YBCO and vice versa. To date, $PrBa_2Cu_3O_7$,[4,5] $Y_xPr_{1-x}Ba_2Cu_3O_7$,[6] normal $YBa_2Cu_3O_x$,[7] and $SrTi_{1-x}Nb_xO_3$[8] have been used as the normal barrier layer in epitaxial SNS type structures. In this letter, we report the use of $CaRuO_3$ as the normal metal layer in YBCO-based SNS junctions.

A candidate barrier layer for epitaxial SNS type structures must satisfy several requirements. First, it has to be an electrically conducting material. Ideally, its metallic conductivity should not depend sensitively on doping, stoichiometry, or oxygen concentration. Second, it should be lattice matched with the YBCO. Finally, its deposition conditions must be compatible with YBCO. A material which satisfies these criteria would also make an excellent resistive element in integrated superconductive circuits made with YBCO in the future.

There are a number of conducting oxides with a perovskite structure; $CaMoO_3$, $LaTiO_3$, $SrRuO_3$, $SrCrO_3$, $SrIrO_3$, and so on. X-ray θ–2θ scans show that the lattice constants in the $(Sr_{1-x}Ca_x)RuO_3$ system range from 3.96 Å for $SrRuO_3$ to 3.86 Å for $CaRuO_3$ when grown as epitaxial films on $LaAlO_3$ substrates. The expanded c-axis lattice constants imply that the films are under compression on $LaAlO_3$ substrates. We have used $SrRuO_3$, $Sr_{0.5}Ca_{0.5}RuO_3$, and $CaRuO_3$ as the barrier layer in SNS junctions and our preliminary results favor $CaRuO_3$. We attribute this to its close lattice match to YBCO and the fact that $SrRuO_3$ has a ferromagnetic transition at 150 K.[9]

$CaRuO_3$ appears to be a well-behaved metallic oxide when it is deposited as an epitaxial film under conditions similar to those used for YBCO. Figure 1 shows the resistivity of an epitaxial $CaRuO_3$ film on a $LaAlO_3$ substrate as a function of temperature. Its resistivity, about 600 $\mu\Omega$ cm at room temperature, decreases as the temperature decreases, implying metallic behavior. However, the curvature of the resistivity versus temperature curve deviates from the traditional Bloch-Gruneissen[10] curve for metals. In addition, there is a large amount of residual resistivity at low temperature. A detailed study of the electomagnetic properties of epitaxial $(Sr_{1-x}Ca_x)RuO_3$ films is underway.

The inset in Fig. 1 displays the geometry of the SNS edge junction we fabricated using laser deposition. First, 2000 Å of epitaxial YBCO and 3000 Å of epitaxial $SrTiO_3$ are deposited on a $LaAlO_3$ substrate. The YBCO/$SrTiO_3$ layer is then patterned by Ar ion beam milling. Next, 100–500 Å of epitaxial $CaRuO_3$ and 2000 Å of epitaxial YBCO are deposited on top of the patterned YBCO/$SrTiO_3$ layer as well as on the etched substrated area. Note that during this step an interface is formed between the $CaRuO_3$ and the previously processed YBCO surface. The $CaRuO_3$/YBCO layer is again patterned by Ar ion beam milling, thereby creating YBCO/$CaRuO_3$/YBCO edge junctions. In order to make contacts to the bottom YBCO, windows in the $SrTiO_3$ layer are etched and the Ag or Au contacts are deposited.

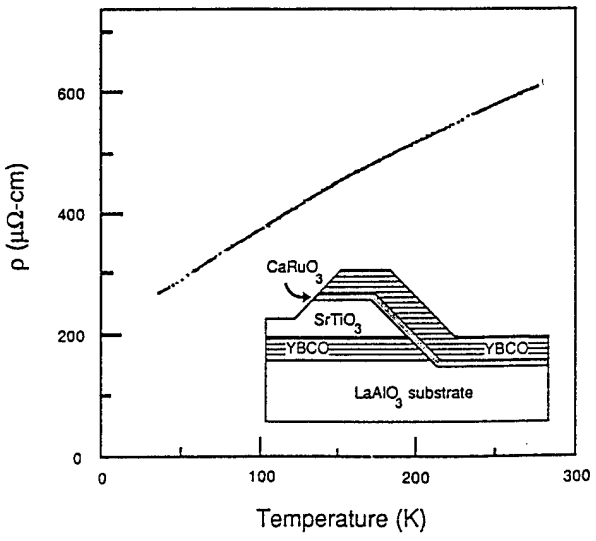

FIG. 1. Resistivity vs temperature curve of epitaxial $CaRuO_3$ on a $LaAlO_3$ substrate measured by the four point method. Inset shows a schematic cross-sectional drawing of the edge junction geometry.

[a]Also at the Department of Applied Physics, Stanford University, Stanford, CA 94305.

 0003-6951/93/020196-03$06.00

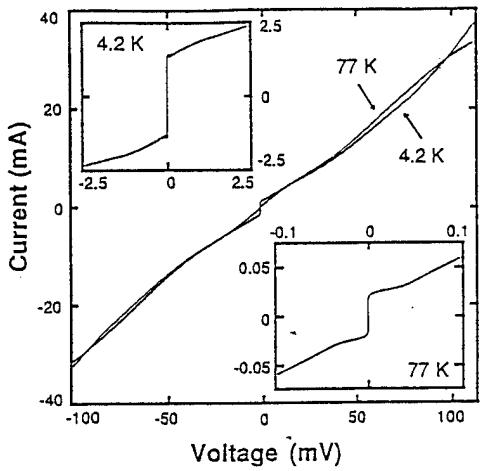

FIG. 2. Current-voltage curves of an YBCO/300 Å $CaRuO_3$/YBCO edge junction at high bias at 77 and 4.2 K. Insets show same current-voltage curves at low bias.

In order to establish the quality of the patterned edge of the first YBCO layer, we made the same junction structure but without the $CaRuO_3$ barrier layer. The critical current density of this YBCO to YBCO structure was higher than 1×10^6 A/cm^2 at 77 K. This implies that most of the ion beam damage done during the initial patterning is annealed out when the YBCO is heated again in 100 mTorr of oxygen for the subsequent deposition.

The current-voltage curves of a junction with a 300 Å $CaRuO_3$ barrier are shown in Fig. 2. At 4.2 K the 10-μm-wide junction shows slightly hysteretic behavior with a 1.3 mA critical current. As we increase the current, the characteristic bends slightly towards a lower dynamic conductance state at voltages near one mV and eventually bends back to a higher conductance state at tens of mV. This behavior of increasing conductance as a function of bias current does not agree with the resistively shunted junction model. This increasing conductance was observed for all the junctions with a barrier thickness from 100 to 500 Å. Whether this peculiar high bias behavior is from the nonlinear current-voltage relation of the $CaRuO_3$ barrier itself or from the properties of the interface between YBCO and $CaRuO_3$ remains to be investigated further, but we note that the junction resistance is predominantly that of the interface. We also would like to note that this increasing conductance has been observed in YBCO tunnel junctions by several groups.[11] As the temperature is increased, the bending in the current-voltage curve becomes smaller. The bending towards a higher resistance state at the 30 mA bias level at 77 K is due to exceeding the critical current of the YBCO current leads.

The effect of the $CaRuO_3$ barrier thickness on junction critical current and resistance was measured. The results at 4.2 K, shown in Fig. 3, exhibit a large scatter at each thickness. The critical current density can be fitted with an exponential relation $J_c(d)=J_{c0}\exp(-d/41\text{ Å})$, suggesting a normal coherence length of 41 Å for $CaRuO_3$ at 4.2 K. The data of normalized junction resistance R_nA show extremely large scatter, with the lowest values still a factor

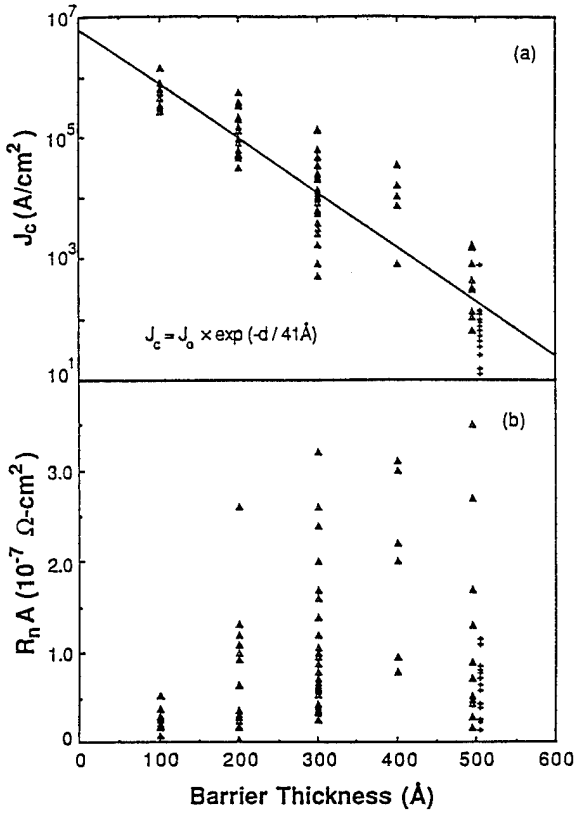

FIG. 3. (a) J_c and (b) R_nA of YBCO/$CaRuO_3$/YBCO junctions as a function of barrier thickness at 4.2 K. Triangles: edge junctions, crosses: trilayer junctions.

of 10 higher than the value calculated from the bulk resistivity shown in Fig. 1. For example, when the thickness of the $CaRuO_3$ barrier is 500 Å, the expected value of $R_nA=\rho_n d=2\times10^{-4}\ \Omega\text{ cm}\times5\times10^{-6}\text{ cm}=10^{-9}\ \Omega\text{ cm}^2$.

There are several candidates for the origin of this extra resistance. Since the edge of the first YBCO electrode was processed *ex situ*, contamination on that surface is a possibility, even though the direct YBCO to YBCO contact had high J_c, as described earlier. In order to answer this question, we fabricated YBCO/500 Å $CaRuO_3$/YBCO trilayer structures with both *c*-axis oriented YBCO and with *a*-axis YBCO. Though all the junction interfaces were made entirely *in situ*, in both cases, regardless of the orientation of the YBCO, the junction reistances were still a factor of 10 higher than the value expected from the bulk resistivity. Another possibility is that, at the interface, there are oxygen depleted regions due to the difference in chemical potential for oxygen in the two different materials, YBCO and $CaRuO_3$. There can also be an intrinsic interface resistance originating from the mismatch in carrier densities and Fermi velocities.[12] The extra resistance would then be similar to the Schottky barrier at semiconductor-metal interfaces. In order to have better control of junction critical currents and resistances, a better understanding of the origin of the extra resistance will be necessary.

Shapiro steps, as well as critical current modulation as a function of mirowave field strength, have been observed. Modulation of critical current in a magnetic field perpen-

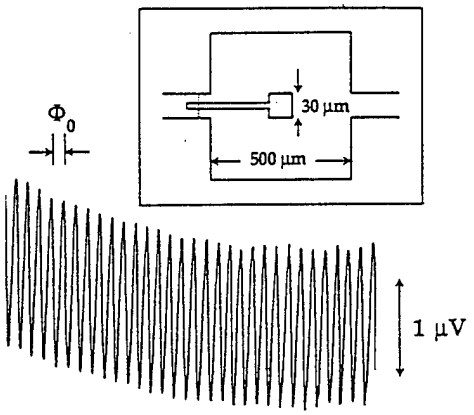

FIG. 4. Voltage modulation of a dc SQUID made with YBCO/200 Å $CaRuO_3$/YBCO edge junctions. Inset shows the planar geometry of the SQUID.

dicular to the substrate shows complicated behavior due to the geometry of edge junctions. A dc SQUID was fabricated with YBCO/200 Å $CaRuO_3$/YBCO junctions. The inset in Fig. 4 shows the planar geometry of the dc SQUID with about 200 pH inductance. At 77 K, the SQUID had a critical current of 600 μA and a resistance of 0.1 Ω. The SQUID showed voltage modulation by magnetic field and its effective area of 16 000 μm^2 agreed well with its geometry.

In summary, we fabricated epitaxial SNS junctions using $CaRuO_3$ as the metallic barrier in the edge junction geometry. The dependence of junction critical current density on the barrier thickness seems to follow an exponential relation with a large scatter. We believe this large scatter in critical current density is related to the junction resistances that are always a factor of 10–100 higher than the bulk resistance of the barrier material. In addition, the current-voltage characteristics show large deviation from the resistively shunted junction model, especially at high bias current.

We would like to thank Laura King and Art Sleight at Oregon State University for providing the $(Sr_{1-x}Ca_x)RuO_3$ materials. We also appreciate the technical assistance of Elena Corpuz, as well as discussions with John Rowell, Randy Simon, Mac Beasley, and Bob Dynes.

[1] D. B. Schwartz, P. M. Mankiewich, R. E. Howard, L. D. Jackel, B. L. Straughn, E. G. Burkhart, and A. H. Dayem, IEEE Trans. Magn. 25, 1298 (1989).
[2] M. S. DiIorio, S. Yoshizumi, K.-Y. Yang, J. Zhang, and M. Maung, Appl. Phys. Lett. 58, 2552 (1991).
[3] R. H. Ono, J. A. Beall, M. W. Cromar, T. E. Harvey, M. E. Johansson, C. D. Reintsema, and D. A. Rudman, Appl. Phys. Lett. 59, 1126 (1991).
[4] C. T. Rogers, M. S. Hedge, B. Dutta, X. D. Wu, and T. Venkatesan, Appl. Phys. Lett. 55, 2032 (1989); J. B. Barner, C. T. Rogers, A. Inam, R. Ramesh, and S. Bersey, Appl. Phys. Lett. 59, 1629 (1991).
[5] J. Gao, W. A. M. Aarnink, G. J. Gerritsma, D. Veldhuis, and H. Rogalla, IEEE Trans. Magn. 27, 3062 (1991).
[6] E. Polturak, G. Koren, D. Cohen, E. Aharoni, and G. Deutscher, Phys. Rev. Lett. 67, 3038 (1991).
[7] B. D. Hunt, M. C. Foote, and L. J. Bajuk, Appl. Phys. Lett. 59, 982 (1991).
[8] D. K. Chin and T. Van Duzer, Appl. Phys. Lett. 58, 753 (1991).
[9] J. M. Longo, P. M. Raccah, and J. B. Goodenough, J. Appl. Phys. 39, 1327 (1968).
[10] See, for example, J. M. Ziman, *Principles of the Theory of Solids* (Cambridge University, Cambridge, 1972), p. 225.
[11] See, for example, M. Gurvitch, J. M. Valles, Jr., A. M. Cucolo, R. C. Dynes, J. P. Garno, L. F. Schneemeyer, and J. Waszejak, Phys. Rev. Lett. 63, 1008 (1989).
[12] M. Yu. Kupriyanov and K. K. Likharev, IEEE Trans. Magn. 27, 2460 (1991).

Josephson coupling of $YBa_2Cu_3O_{7-x}$ through a ferromagnetic barrier $SrRuO_3$

L. Antognazza,[a] K. Char, and T. H. Geballe[a]
Conductus, Inc., 969 West Maude Avenue, Sunnyvale, California 94086

L. L. H. King and A. W. Sleight
Department of Chemistry, Oregon State University, Corvallis, Oregon 97331

(Received 24 May 1993; accepted for publication 17 June 1993)

Epitaxial barriers of ferromagnetic $SrRuO_3$ have been used to fabricate high T_c superconductor-normal-superconductor Josephson junctions in the edge junction geometry. At small barrier thicknesses the $SrRuO_3$ junctions follow the behavior of nonferromagnetic but otherwise closely related $CaRuO_3$ junctions. A rapid disappearance of critical current is observed when the barrier thickness is increased to 250 Å. Possible origins of such a large critical thickness are discussed.

In our recent study of superconductor-normal-superconductor (SNS) Josephson junctions using epitaxial metallic oxide $CaRuO_3$ as the barrier layer,[1] we identified several other candidate barrier materials including the $(Ca_xSr_{1-x})RuO_3$ system. In this system, it has been shown[2,3] that $SrRuO_3$ undergoes ferromagnetic ordering at temperatures between 150 and 160 K, while $CaRuO_3$ is nonmagnetic. Theoretical treatments of superconductor-ferromagnetic-superconductor (SFS) junctions have been made over the years.[4,5] A critical thickness of a ferromagnetic barrier, above which there is no overlap of superconducting wave functions and hence zero Josephson current, is predicted by Kuplevakhskiĭ and Fal'ko.[4] On the other hand Buzdin *et al.* reported an oscillation of the critical current of the junction with the ferromagnetic barrier thickness.[5] Experiments on low T_c Pb-Fe-Pb junctions by Claeson[6] indicate a critical thickness of 5 Å. This small value may be due to efficient pair breaking by spin flip scattering at the interfaces as well as the magnetization of Fe.

In the case of high T_c material systems, study of SFS structures is all the more interesting since high T_c superconductivity is generally believed to originate from a magnetic background state. Kasai *et al.*[7] reported the observation of supercurrents in trilayer junctions with a 5000-Å-thick $La_{0.7}Ca_{0.3}MnO_z$ ferromagnetic barrier. No follow-up confirmation of this work, for which there is no reasonable physical model, has been reported to our knowledge. In this letter we report electrical characteristics of SFS-type Josephson junctions made with $YBa_2Cu_3O_{7-x}$ (YBCO) as electrodes and $SrRuO_3$ as the barrier layer in the edge junction geometry.

When grown epitaxially on $LaAlO_3$ substrates, $SrRuO_3$ has the lattice constant of 3.96 Å in the growth direction. The expanded *c*-axis lattice constant may imply that the films are under compression on $LaAlO_3$ substrates. The temperature dependence of resistivity of an epitaxial $SrRuO_3$ film on $LaAlO_3$ is shown in Fig. 1. The cusp at 150 K is presumably due to a decrease in spin flip scattering when $SrRuO_3$ undergoes ferromagnetic ordering. The magnetic ordering in $SrRuO_3$ is believed to be either canted or itinerant ferromagnetism, and results in a moment of about 1 μ_B per Ru atom.[2,3,8] It is important to note that exactly the same temperature dependence and cusp in the resistivity is maintained even for the 100-Å-thick $SrRuO_3$ films on $LaAlO_3$ substrates, which indicates that 100-Å-thick $SrRuO_3$ films maintain a Curie temperature at 150 K.

The YBCO/$SrRuO_3$/YBCO junctions were fabricated by the same process as that used for YBCO/$CaRuO_3$/YBCO junctions.[1] Epitaxial layers were grown by laser ablation and all the patterning was done by Ar ion beam milling. According to cross-sectional scanning electron microscope studies, the angle of the slope of the first YBCO edge is about 20°. In order to avoid shorts in the nonbarrier regions an epitaxial $SrTiO_3$ layer or polycrystalline MgO layer was used as the isolation layer between the first and second YBCO electrodes.

In order to assess the quality of the edge of the first YBCO, junction structures were made without any barrier layer. All the structures showed critical current densities higher than 1×10^6 A/cm^2 at 77 K. They did not show any weak link behavior even at temperatures very close to the transition temperatures of the YBCO electrodes, which is usually between 87 and 90 K. On the other hand, several edge junction structures were made and tested with an

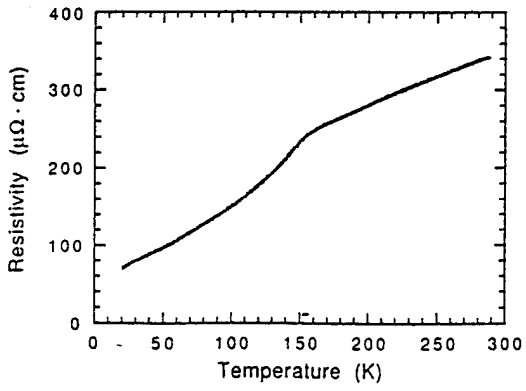

FIG. 1. Temperature dependence of resistivity for a 3000-Å-thick $SrRuO_3$ thin film on a $LaAlO_3$ substrate.

[a]Also at Department of Applied Physics, Stanford University, Stanford, CA 94305.

 0003-6951/93/63(7)/1005/3/$6.00

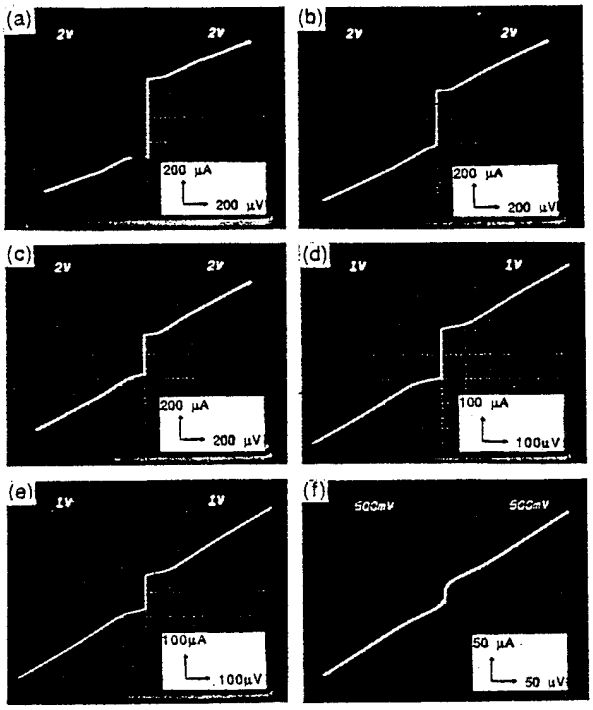

FIG. 2. I-V curves of a 5-μm-wide junction with 200-Å-thick $SrRuO_3$ barrier at (a) 4.2 K, (b) 28.8 K, (c) 45 K, (d) 56.5 K, (e) 63.7 K, and (f) 73.3 K.

insulating $SrTiO_3$ barrier layer. As long as the $SrTiO_3$ barrier layer was thicker than 100 Å, there was no critical current, even though the resistance of the structures varied from tens of ohms to hundreds of kilo-ohms. When the $SrTiO_3$ barrier was 50-Å thick, we observed fairly large zero resistance currents which we attribute to microshorts through the barrier layer.

The current-voltage (I-V) curves of a 5-μm-wide YBCO/200 Å $SrRuO_3$/YBCO junction at several temperatures are shown in Fig. 2. At 4.2 K the critical current shows a small hysteresis with 320 μA critical current. The junction also exhibits a slight hump in its I-V characteristic around 400 μV. The I-V curve at higher bias, around tens of mV, shows the increase of conductance, as was the case for the $CaRuO_3$ barriers.[1] We believe that this increasing conductance results from interface properties between the YBCO and $SrRuO_3$, as in YBCO/$CaRuO_3$ interfaces. The features of the hump and increasing conductance at high bias disappear as the temperature increases. At 77 K the I-V curve shows nonlinear behavior due to thermally activated phase slip in the junction and there is no zero resistance current.

The temperature dependence of critical current and resistance of the junction is displayed in Fig. 3. The critical current disappears linearly as the critical temperature is approached. Even though the temperature dependence cannot be accurately fit to a power law relation $I_c \propto (T_c - T)^n$ near the critical temperature due to thermally activated phase slip, $n=1$ is a good fit over most of the range. The junction resistance R_n increases slightly as the junction is cooled down. We note, however, that the resistance of junctions at low temperatures can only be approximately

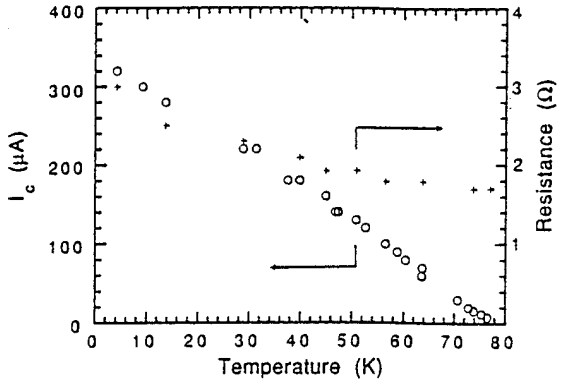

FIG. 3. Temperature dependence of I_c and R_n of a 5-μm-wide junction with 200-Å-thick $SrRuO_3$ barrier.

defined because there are large deviations in the I-V characteristics from the resistively shunted junction model. It should also be noted that the resistance of the junction is an order of magnitude higher than is expected from the bulk properties of $SrRuO_3$, and thus interface resistance is important. The temperature dependence of the critical current and the resistance of the junction is similar to that of grain boundary junctions of YBCO,[9] which leads us to speculate that the temperature dependence may be a general property of YBCO interfaces.

In Fig. 4 the thickness d dependence of J_c and $R_n A$, where A is the area of the junction, at 4.2 K are shown for all the samples measured over the past year in this study. The large scatter is attributed to the variation of the nominal barrier thickness which was estimated from the deposition time, and to the barrier uniformity. The runs made

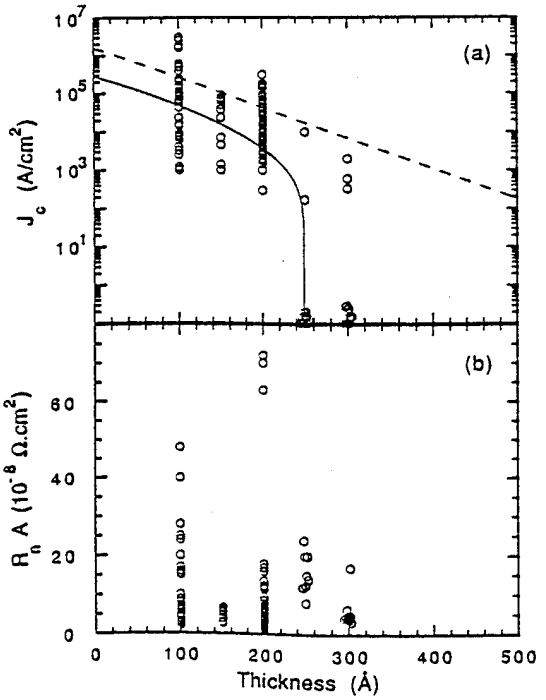

FIG. 4. (a) J_c and (b) $R_n A$ as a function of barrier thickness at 4.2 K. In (a) the dashed line represents the fit for the $CaRuO_3$ junctions and the solid line is the fit using Eq. (1) with $J_0=2.9\times10^5$ (A/cm^2), $\xi_n=62$ Å, and $d_c=250$ Å.

during the early part of this investigation also had higher interface resistances. The dashed line represents the average behavior of YBCO/$CaRuO_3$/YBCO junctions as reported in Ref. 1. At small d, the critical current density seems to follow that of $CaRuO_3$ barrier junctions, even though the average value is slightly lower for the ferromagnetic $SrRuO_3$ barrier. When the $SrRuO_3$ thickness is equal or above 250 Å, 24 of the 29 junctions measured showed no critical current. Thus 250 Å seems to be a critical thickness above which the critical current vanishes. A possible trivial explanation for this large critical thickness, namely that the $SrRuO_3$ barrier material is not ferromagnetic when it is thinner than 250 Å, is inconsistent with the 100-Å-thick $SrRuO_3$ films having the same temperature dependence of resistivity as the thick films and bulk, as previously noted. However, we cannot at present exclude the possibility that the thin $SrRuO_3$ barrier grown at the edge of YBCO is not ferromagnetic due to epitaxial or thermal stress, although it is unlikely. Considering the low angle of the slope of the edge, we believe the thickness of the $SrRuO_3$ barrier in the edge junction geometry is not much different from the thickness of $SrRuO_3$ films deposited on a flat substrate. The thickness dependence of R_nA in Fig. 4(b) again suggests the importance of interface resistances in YBCO/$SrRuO_3$ structures. In fact the interface resistance of $SrRuO_3$ barrier junctions are slightly higher than that of $CaRuO_3$ barrier junctions, which could result from the slightly larger lattice mismatch in YBCO/$SrRuO_3$ structures. In addition the large critical thickness indicates the lack of pair-breaking scattering at the interface by magnetic moment.

The solid curve in Fig. 4(a) is a fit to the data using the equation of Ref. 4 for the critical current as a function of barrier thicknesses,

$$J_c = J_0 \exp(-d/\xi_n)\,[1-2\sin^2(\pi d/4d_c)], \qquad (1)$$

where ξ_n is the coherence length, D the diffusion constant in the F material, and $d_c = 5\pi/4\ (\hbar D/k_B T_{\text{curie}})^{1/2}$ is the critical thickness above which there is no Josephson coupling. The first factor is the usual exponential decay and the second accounts for the opposite precession of the up and down spin inside the ferromagnetic barrier. This is derived with the assumption of negligibly small spin orbit scattering and that the exchange energy $h = k_B T_{\text{curie}}$ is greater than $k_B T_c$. The equation is valid near T_c and it remains to be seen how well it works at low temperatures. Our fitting parameters are $\xi_n = 62$ Å for the exponential decay, a reasonable value compared to the 44 Å found for $CaRuO_3$ barriers in Ref. 1, and the critical thickness $d_c = 250$ Å. Here if we take $T_{\text{curie}} = 150$ K, the diffusion constant D comes out to be 8 cm^2/s, not an unreasonable value.

The 200 Å junction was also tested in a magnetic field and under microwave radiation. When the magnetic field was applied in the direction perpendicular to the substrate, the pattern obtained from the modulation of voltage as a function of magnetic field is more like that of a SQUID than that of a uniform single junction, suggesting nonuniformity of the critical current density. Microwave irradiation at higher temperature almost completely suppressed the critical current, but none of the $SrRuO_3$ junctions showed the Shapiro steps. However, the critical current was modulated as a function of microwave power. It is not clear whether the interface or the ferromagnetism is responsible for the nonideal properties of the junction under microwave radiation. However, the fact that we do observe Shapiro steps in $CaRuO_3$ barrier junctions, even though they are not as well defined as those from biepitaxial grain boundary junctions,[9,10] suggests that ferromagnetism may be involved. Further, a nontrivial current phase relationship is predicted in Ref. 4 for ferromagnetic barriers making the behavior of the junction under microwave complicated.

In summary, we report the electrical properties of SNS-type Josephson junctions based on YBCO with $SrRuO_3$ barrier layers. We observe a critical thickness of 250 Å for the $SrRuO_3$ barrier layer, above which the critical current vanishes abruptly. A small possibility exists that the large critical thickness is the result of loss of ferromagnetic ordering in the thinner barriers or a change of intrinsic properties due to the high T_c materials in proximity with a ferromagnetic barrier. We observe large interface resistances, as in the case of $CaRuO_3$ barriers, and an unusual behavior of the junction under microwave radiation. However, we were able to fit the data with reasonable parameters to a theory developed for SFS junctions.

We would like to thank Mac Beasley, Bob Dynes, John Rowell, and Yuri Suzuki for helpful discussions and Elena Corpuz for her technical assistance. Part of this work at Conductus was supported by a Small Business Innovative Research contract by the Strategic Defense Initiative Organization. The work at Oregon State University and at Stanford University was supported in part by the Air Force Office of Scientific Research. One of us (L.A.) would like to thank the support of "Fond National Suisse de la Recherche Scientifique."

[1] K. Char, M. S. Colclough, T. H. Geballe, and K. E. Myers, Appl. Phys. Lett. 62, 196 (1993).
[2] A. Callaghan, C. W. Moeller, and R. Ward, Inorg. Chem. 5, 1572 (1966).
[3] A. Kanabayasi, J. Phys. Soc. Jpn. 41, 1876 (1976); see also, P. A. Cox, R. G. Egdell, J. B. Goodenough, A. Hammett, and C. C. Naish, J. Phys. C 16, 6221 (1983).
[4] S. V. Kuplevakhskiĭ and I. I. Fal'ko, Teor. Mat. Fiz. 86, 272 (1991); S. V. Kuplevakhskiĭ and I. I. Fal'ko, *ibid.* 84, 146 (1989).
[5] A. I. Buzdin and M. Yu. Kupriyanov, JETP Lett. 53, 322 (1991).
[6] T. Claeson, Thin Solid Films 66, 151 (1980).
[7] M. Kasai, T. Ohno, Y. Kanike, Y. Kozono, M. Hanazono, and Y. Sugita, Jpn. J. Appl. Phys. 29, 2219 (1990).
[8] C. B. Eom, R. J. Cava, R. M. Fleming, J. M. Philipps, R. B. van Dover, J. H. Marshall, J. W. P. Hsu, J. J. Krajewski, and W. F. Peck, Jr., Science 258, 1766 (1992).
[9] K. Char, M. S. Colclough, L. P. Lee, and G. Zaharchuk, Appl. Phys. Lett. 59, 2177 (1991).
[10] E. A. Early, A. F. Clark, and K. Char, Appl. Phys. Lett. 62, 3357 (1993).

Study of interface resistances in epitaxial $YBa_2Cu_3O_{7-x}$/barrier/$YBa_2Cu_3O_{7-x}$ junctions

K. Char
Conductus, Inc., Sunnyvale, California 94086

L. Antognazza and T. H. Geballe
Department of Applied Physics, Stanford University, Stanford, California 94305

(Received 14 July 1993; accepted for publication 25 August 1993)

We have measured interface resistances in $YBa_2Cu_3O_{7-x}$/barrier/$YBa_2Cu_3O_{7-x}$ junctions with different barrier materials in an edge junction geometry. $CaRuO_3$, $La_{0.5}Sr_{0.5}CoO_3$, $Y_{0.7}Ca_{0.3}Ba_2Cu_3O_{7-x}$, $YBa_2Cu_{2.79}Co_{0.21}O_{7-x}$, and $La_{1.4}Sr_{0.6}CuO_4$ have been employed as the epitaxial barrier materials. We observe interface resistances of the order of 1×10^{-8} Ω cm^2 when we use $CaRuO_3$ and $La_{0.5}Sr_{0.5}CoO_3$ barriers. These two barrier materials are cubic perovskites. However, in the case of the layered barrier materials, the measured interface resistances are smaller than 1×10^{-10} Ω cm^2. Our study suggests that the oxygen disorder at the $YBa_2Cu_3O_{7-x}$ surface, due to stress created by the thermal expansion mismatch between $YBa_2Cu_3O_{7-x}$ and the barrier, may be the origin of the interface resistances, and that the magnitude of this stress can change the resistance by orders of magnitude.

The emerging electronics technology based on high-T_c superconductors is limited at present by our understanding of the materials themselves, particular when the superconductors are integrated into circuits. Central to advances in the processing of these oxide materials in multilayer devices and circuits is an understanding of the properties of interfaces between the oxides and other materials. Examples are the interfaces of superconductors with normal metals such as Ag or Au, with normal epitaxial oxide metals used as resistors and barrier layers in superconductor-normal-superconductor (SNS) junctions, with insulating oxides in crossovers, and with other superconducting films in via contacts. For example, in SNS junctions utilizing Ag, Au,[1,2] or $CaRuO_3$ (Ref. 3) as the N layer, the junction resistance is dominated by the interface resistance rather than the bulk resistance of the normal metal. Lack of control of this interface resistance leads to large nonuniformities in junction properties across the wafer and probably within the individual junctions. As far as we know, this has been true for all SNS junctions made of the oxide materials. As the SNS junction is becoming important in high-T_c superconducting quantum interference devices (SQUIDs) and single flux quantum (SFQ) digital circuits, it is essential to be able to understand and control this interface resistance.

Recently in epitaxial SNS junctions with an epitaxial $CaRuO_3$ barrier,[3] we identified the important role the interface resistance plays in determining the critical parameters of junctions such as critical current density (J_c) and normalized resistance (R_nA). In this letter we present the measurement of interface resistances of $YBa_2Cu_3O_{7-x}$ (YBCO)/barrier/YBCO edge junctions with five different epitaxial barriers. In order to elucidate the origin of interface resistances, we chose the metallic barrier materials to have a rather wide range of properties, as we considered that the interface resistance might be due to mismatches in carrier density, lattice constant, thermal expansion, and dimensionality.

The lattice constants and thermal expansion coefficients of YBCO, $SrTiO_3$, $LaAlO_3$, and five barrier materials are listed in Table I. We used two cubic perovskite barrier materials $CaRuO_3$ and $La_{0.5}Sr_{0.5}CoO_3$ as well as three layered materials $Y_{0.7}Ca_{0.3}Ba_2Cu_3O_{7-x}$, $YBa_2Cu_{2.79}Co_{0.21}O_{7-x}$, and $La_{1.4}Sr_{0.6}CuO_4$. We would like to emphasize the large difference in thermal expansion coefficients between the YBCO along the c axis and the cubic perovskite barriers.

The schematics and processing procedures of our edge junctions are described in Ref. 3. When we made an edge junction structure without any barrier layer, the YBCO/YBCO contacts carried critical current densities higher than 1×10^6 A/cm^2. This suggests that the ion mill damaged YBCO surface restores its crystallinity during the heating for the second barrier/YBCO deposition. On the other hand, when we used 10-nm-thick $SrTiO_3$ layer as the barrier layer, the junction did not show any zero voltage current, even though the resistance of the junctions varied between tens of ohms and hundreds of kilo-ohms.

The first results of junctions made with $CaRuO_3$ bar-

TABLE I. Lattice constants and thermal expansion coefficients of YBCO, $LaAlO_3$, $SrTiO_3$, and barrier materials used in this study.

Materials	Lattice constants (Å)	Expansion coefficients (10^{-6}/°C around 400 °C)
YBCO	3.82–3.89 (a,b)	8–10 (a,b)
	11.7 (c)	17–20 (c)
$LaAlO_3$	3.79	10
$SrTiO_3$	3.90	10
$CaRuO_3$	3.85–3.86	10
$La_{0.5}Sr_{0.5}CoO_3$	3.83–3.84	10
$Y_{0.7}Ca_{0.3}Ba_2Cu_3O_{7-x}$	3.82–3.89 (a,b)	8–10 (a,b)
	11.7 (c)	20 (c)
$YBa_2Cu_{2.79}Co_{0.21}O_{7-x}$	3.82–3.89 (a,b)	8–10 (a,b)
	11.7 (c)	17–20 (c)
$La_{1.4}Sr_{0.6}CuO_4$	3.9 (a)	10 (a)
	13.3 (c)	17–20 (c)

 0003-6951/93/63(17)/2420/3/$6.00

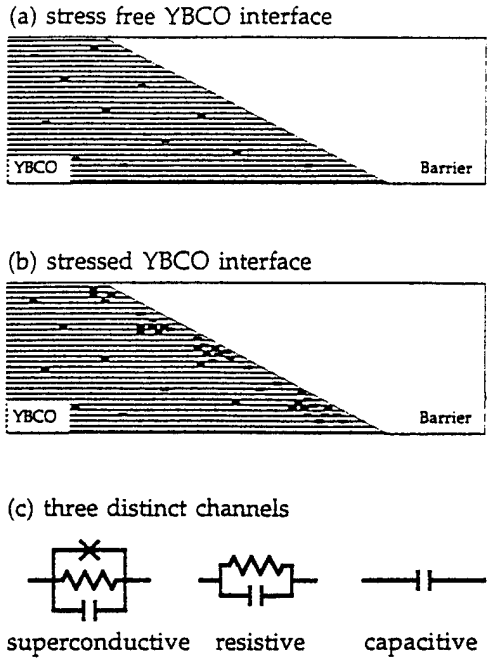

FIG. 2. Schematic drawings of oxygen deficient/disordered states at YBCO/barrier (a) in the case of good thermal match and (b) in the case of poor thermal match. (c) Representations of three different channels in SNS type junctions depending on the microscopic density of localized states at the interface.

interface resistance between YBCO and the $La_{1.4}Sr_{0.6}CuO_4$ barrier.

The interface resistance observed for $CaRuO_3$ and $La_{0.5}Sr_{0.5}CoO_3$ barriers has a very similar temperature dependence to that of high angle grain boundaries of YBCO,[9] as does its critical current. In addition, the magnitude of the interface resistance, about $1\times10^{-8}\ \Omega\ cm^2$, is also comparable to that of high angle grain boundaries of YBCO. Even though we cannot completely rule out the possibility of chemical reaction at the interface, the similarity of magnitude and temperature dependence of the interface resistance points towards some sort of oxygen deficiency/disorder at the YBCO interface as the origin of the interface resistance. This is now generally believed to be the origin of the resistance of grain boundaries. The density of oxygen deficiency/disorder at the interface could easily be enhanced at the YBCO interface in the case of barriers with poor thermal match, since the YBCO surface cannot absorb enough oxygen and contract its *c* axis during the cool down.

In Fig. 2 we show our schematic description of the oxygen deficient/disordered states at YBCO/barrier interfaces. In the case of barriers with a good thermal match with the YBCO *c* axis, the density of oxygen deficient/disordered states at the interface is not much different from that in the bulk of the YBCO. However, the density of oxygen deficient/disordered states is higher at the interface in the case of barriers with poor thermal match, resulting in significant interface resistances. If these oxygen deficient/disordered states tend to cluster together, as shown by recent electromigration experiments,[10] there will exist a modulation of the density of localized states across the junction interfaces, as shown in Fig. 2(b). Depending on the density of localized states at the interface, the local microscopic junction area will then behave as a superconductive channel that carries phase coherent Josephson current, a resistive channel that carries normal shunt current but no supercurrent, and a capacitive channel that does not carry any significant dc current.

In summary, we have reported the interface resistances in SNS junctions between YBCO and five different epitaxial barriers. The similarity of interface resistance to that of grain boundaries of YBCO in the case of barriers with poor thermal match and the absence of interface resistance in the case of well thermally matched barriers suggest that the clustering of oxygen deficient/disordered localized states at the interface may be the origin for the interface resistance. We believe these experiments are the first steps towards engineering the oxide interfaces in SNS junctions and multilayer circuits in general. As we understand the origin of the interface resistance better, we expect to have improved control over the interface resistance, which will eventually lead to an epitaxial SNS Josephson junction technology with improved uniformity of resistance and critical current.

We would like to thank Elena Corpuz for her very valuable technical assistance and John Rowell for helpful discussions on this work. We acknowledge discussions on this subject with Brian Moeckly and Bob Burhman of Cornell University. We also would like to thank Laura King and Art Sleight at Oregon State University for providing several barrier materials.

[1] M. S. DiIorio, S. Yoshizumi, K.-Y. Yang, J. Zhang, and M. Maung, Appl. Phys. Lett. 58, 2552 (1991).
[2] R. H. Ono, J. A. Beall, M. W. Cromar, T. E. Harvey, M. E. Johansson, C. D. Reintsema, and D. A. Rudman, Appl. Phys. Lett. 59, 1126 (1991).
[3] K. Char, M. S. Colclough, T. H. Geballe, and K. E. Myers, Appl. Phys. Lett. 62, 196 (1993).
[4] J. T. Cheung, P. E. D. Morgan, D. H. Lowndes, X.-Y. Zheng, and J. Breen, Appl. Phys. Lett. 62, 2045 (1993).
[5] Y. Tokura, J. B. Torrance, T. C. Huang, and A. I. Nazzal, Phys. Rev. B 38, 7156 (1988).
[6] A. Carrington, A. P. Mackenzie, C. T. Lin, and J. R. Cooper, Phys. Rev. Lett. 69, 2855 (1992).
[7] G. G. Li, F. Bridges, J. B. Boyce, and W. C. H. Joiner, Phys. Rev. B 47, 12110 (1993); R. S. Howland, T. H. Geballe, S. S. Laderman, A. Fisher-Colbrie, M. Scott, J. M. Tarascon, and P. Barboux, Phys. Rev. B 39, 9017 (1989).
[8] H. Takagi, T. Ido, S. Ishibashi, M. Uota, S. Uchida, and Y. Tokura, Phys. Rev. B 40, 2254 (1989).
[9] K. Char, M. S. Colclough, L. P. Lee, and G. Zaharchuk, Appl. Phys. Lett. 59, 2177 (1991).
[10] B. H. Moeckly, D. K. Lathrop, and R. A. Buhrman, Phys. Rev. B 47, 400 (1993).

Noise characteristics of $YBa_2Cu_3O_{7-\delta}/CaRuO_3/YBa_2Cu_3O_{7-\delta}$ Josephson junctions

K. E. Myers,[a),b)] K. Char, M. S. Colclough, and T. H. Geballe[b)]
Conductus, Inc., Sunnyvale, California 94086

(Received 7 September 1993; accepted for publication 16 November 1993)

The noise characteristics of $YBa_2Cu_3O_{7-\delta}/CaRuO_3/YBa_2Cu_3O_{7-\delta}$ edge junctions are reported. The junctions exhibit low $1/f$ noise in the range of operating temperatures from 65 to 77 K. At lower temperatures the level of $1/f$ noise increases, and in addition, telegraph noise dominates the noise power spectrum at discrete current biases that are junction dependent. The characteristic frequency of a particular switching process increases with temperature but may increase or decrease with increased bias current. These results are consistent with a description of the superconductor-metal interface in which oxygen deficiency and/or disorder gives rise to localized states which trap carriers and lead to noise in the junction transmission.

In recent letters,[1,2] we have identified the importance of the interface between $YBa_2Cu_3O_{7-\delta}$ (YBCO) and other epitaxial metal oxides in determining the properties of superconductor-normal metal-superconductor (SNS) junctions made of those materials. For certain normal metals, including $CaRuO_3$ (CRO), the resistances of SNS junctions made with YBCO are dominated by interface resistance. In an effort to isolate the origin of the YBCO/CRO interface resistance, we have studied the noise properties of YBCO/CRO/YBCO junctions as a function of temperature and bias current.

There have been several papers describing the noise characteristics of grain boundary junctions, and superconducting quantum interference devices (SQUIDs), fabricated from YBCO[3–7] and thallium-2212[8] thin films. In most of these studies, the noise power spectrum was found to have a $1/f$ frequency dependence.[9] For normal metal-insulator-metal junctions, Rogers and Buhrman have shown that the typically observed $1/f$ noise spectrum is actually an aggregate of single Lorentzian spectra, each due to the trapping and escape of carriers at a localized state in the barrier, but with a distribution of lifetimes.[10] A similar mechanism is expected to be at the heart of $1/f$ noise in both high T_c grain boundary and SNS junctions. However, in previous work, the individual Lorentzian spectra were not resolved so that information regarding the localized states could not be extracted.

The current-voltage characteristics of the YBCO/CRO/YBCO junctions used in this study were described previously.[1] One of the major results of that work was that the junction resistance was two orders of magnitude higher than expected on the basis of the resistivity and dimensions of the CRO layer, and was independent of CRO thickness. It was asserted that there must be some sort of insulating barrier between the CRO and YBCO. By studying the noise characteristics of YBCO/CRO/YBCO junctions, and in concert with a study of YBCO SNS junctions with different normal metals,[2] we have developed a description of the superconductor-metal interface in which oxygen deficiency and/or disorder gives rise to localized states which trap carriers and lead to voltage noise and high resistance across the junction.

SNS junctions in the step-edge geometry were fabricated using laser deposition. First, 2000 Å of epitaxial YBCO and 3000 Å of epitaxial $SrTiO_3$ are deposited on a $LaAlO_3$ substrate. The YBCO/$SrTiO_3$ bilayer is then patterned by Ar ion beam milling. Next, 100–200 Å of epitaxial CRO and 2000 Å of YBCO are deposited on top of the patterned bilayer as well as on the etched substrate area. The CRO/YBCO bilayer is patterned by Ar ion beam milling, thereby creating YBCO/CRO/YBCO edge junctions. In order to make contacts to the bottom YBCO layer, windows are etched through the $SrTiO_3$ layer, and Ag or Au contacts are deposited. The critical currents of the 6 and 10 μm wide junctions included in this study are, at 4.2 K, between 2.4 and 5.0 mA and the resistances are between 1.2 and 2.0 Ω.

The samples are patterned into a four-point geometry. An HP 3312A Signal Generator provides a constant current using a large ballast resistor. The measured voltage noise is independent of the value of that resistor, eliminating current source noise as a possible source of voltage noise. The voltage across the junction is directed to a low-noise preamplifier and is then frequency analyzed by an HP 35660A Dynamic Signal Analyzer while time traces are taken with an HP 54501A Digitizing Oscilloscope. All measurements are taken with the sample inside a high-permeability metal shield and in a rf-shielded room. The white noise floor of this apparatus was about 3 nV/√Hz referred to the sample. We note that our first measurements were done in a system with a much lower noise floor, but we found that such careful measurements were unnecessary.

In Fig. 1 we show the voltage noise power, $S_v^{1/2}$, at 10 Hz for several junctions at their highest operating temperature as a function of the bias current I_b. The noise in the 10 μm junctions is about 2 nV/√Hz (above the noise floor) at 10 Hz when biased just above the critical current, I_c. This is comparable to the voltage noise measured for YBCO grain boundary junctions. The noise level for the 6 μm junction (C) is, at high biases, larger by a factor of nearly 2 than

[a)]Current address: Du Pont Central Research and Development, Experimental Station, P.O. Box 80304, Wilmington, DE 19880-0304.
[b)]Also at the Department of Applied Physics, Stanford University, Stanford, CA 94305.

 0003-6951/94/64(6)/788/3/$6.00

that of the 10 μm wide junctions (A and B) as expected. At all bias currents above I_c, the noise has a $1/f$ frequency dependence as seen, for example, in the inset of Fig. 1. The low $1/f$ noise of these junctions at the junction operating temperatures makes them potentially useful in various applications.

Following Kawasaki *et al.*,[4] we expect that the main contribution to the voltage noise across a given junction is from transmission fluctuations due to the trapping and release of carriers, as opposed to flux motion, in the junction. The junction transmission fluctuations give rise to both critical current and resistive fluctuations. In a uniform junction the normalized magnitudes of these two noise sources should be the same.[5] These two components of the voltage noise can be distinguished as the critical current fluctuations dominate at I_c while the resistance fluctuations dominate at high bias current. Because the data in Fig. 1 were taken at relatively high temperatures, there is not in all cases a peak in S_v at I_c, making it difficult to determine the level of the critical current fluctuations. However, at high bias we can determine that the normalized resistance fluctuations, $\partial R_n/R_n$, are in the range of $3–7\times10^{-6}/\sqrt{\text{Hz}}$ for all three junctions.

The noise level for a particular junction increases with decreasing temperature. The voltage noise across a 10 μm YBCO/CRO/YBCO junction at 4.2 K is plotted as a function of bias current in Fig. 2. There is a peak in the noise just above the junction critical current ($\approx$2.6 mA). With increasing bias current, the noise drops down to a minimum and then quickly rises again. The noise generally has a $1/f$ power spectrum at low temperature, as at high temperature. In the low-temperature case, we can distinguish the contributions of the critical current and resistance fluctuations. At 4.2 K, the normalized critical current nose, $\partial I_c/I_c$, is about $13\times10^{-5}/\sqrt{\text{Hz}}$ while the normalized resistance noise is half of that value indicating that the junction is relatively uniform. In addition to this noise there is, however, a series of peaks that occur over very narrow bias current regions, and without any corresponding features in the I-V characteristics.

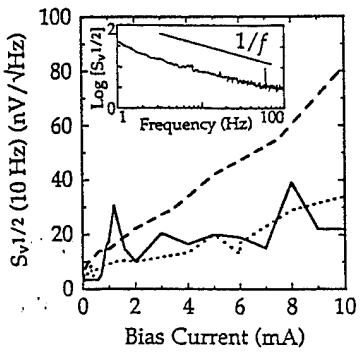

FIG. 1. Voltage noise power (at 10 Hz) as a function of bias current for three YBCO/CRO edge junctions. Solid line: sample A, 10 μm wide, $T=65$ K; dotted line: sample B, 10 μm wide, $T=65$ K; dashed line: sample C, 6 μm wide, $T=77$ K. Inset: Log of the voltage noise power (nV/$\sqrt{\text{Hz}}$) as a function of frequency for sample C at $T=77$ K and $I_b=0.1$ mA. The solid line shows a $1/f$ dependence.

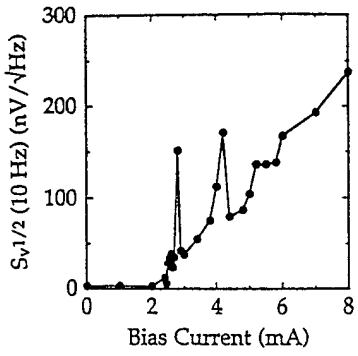

FIG. 2. Voltage noise power (at 10 Hz) as a function of bias current for sample B at $T=4.2$ K. The critical current for the junction is about 2.6 mA at this temperature. Note the peak in the voltage noise just above I_c, but also at $I_b\approx4$ and 5 mA.

For example, the noise power spectrum corresponding to the peak in Fig. 2 at $I_b\approx4$ mA is shown in Fig. 3. In this bias current regime, the power spectrum is dominated by a single Lorentzian, that is, the noise power is flat below a characteristic frequency, and falls as $1/f^2$ at higher frequency. A typical time trace of the voltage noise is shown in the inset to Fig. 3. A random telegraph signal (RTS) is seen clearly; the voltage difference between the two states being approximately 0.5 μV. For this particular peak, the characteristic frequency, or the inverse of the average time between transitions, moves to lower frequency with increased current bias. For different peaks, the opposite behavior is observed. In all cases however, the characteristic frequency increases with increased temperature as would be expected for an activated process. Our earlier assumption that the noise is not primarily due to flux hopping seems to be verified by the fact that the voltage bias at which a given RTS appears does not change with magnetic field environment or with thermal cycling.

In order to explain our observations, we have developed the following picture of YBCO/CRO/YBCO junctions. At the YBCO/CRO interface, there are oxygen deficiencies and/or disorder due to strain between the layered YBCO and

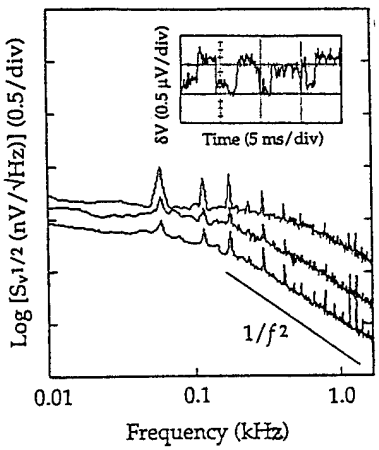

FIG. 3. Log of the voltage noise power as a function of frequency for sample B at $T=4.2$ K. From top to bottom, the traces were taken at $I_b=4.1$, 4.2, and 4.3 mA and are offset for clarity (the peaks at 60 Hz, 120 Hz, etc. are due to line frequency interference). The straight, solid line shows a $1/f^2$ dependence. Inset: A time trace of the voltage fluctuations.

the cubic CRO, possibly as a result of the thermal expansion coefficient mismatch between the two materials.[2] The oxygen defects tend to cluster,[11] leading to insulating regions at the YBCO/CRO interface. As a result, there are at least two different types of interface regions, with different electrical properties. There are superconducting channels corresponding to areas with relatively few defects. There are also resistive channels through more highly defected regions. Additionally, there may be capacitive channels, which would not have an impact on the voltage noise.

There are a large number of superconducting channels, and there are carrier trapping sites in those areas. Any charge trapped in localized states in such a conductive region will be heavily screened and therefore have a small impact on the overall junction transmission. However, the sum of the conductance fluctuations due to all of these states, having a distribution of lifetimes, leads to low-level $1/f$ noise.

Though the number of resistive channels is smaller, trapping of an individual carrier in these regions having relatively long screening lengths has a larger effect on the junction transmission. We suggest that these regions are the source of the large random telegraph signals observed.

In the original Rogers and Buhrman work, it was shown that thermally activated ionic reconfiguration may allow the trapping of a carrier in the barrier resulting in a change in the junction transmission. The barrier energy between the two configurations, most likely related to the motion of an oxygen vacancy, was on the order of meV.[12] For YBCO/CRO/YBCO junctions, we estimate that the energy scale for the RTS is also a few meV, suggesting the role of ionic motion in the switching process. This estimate is based on the fact that for our junctions, the random telegraph signals move to very high frequency, and the amplitudes decrease significantly, at temperatures between 10 and 30 K. Assuming the energy of the barrier to ionic motion, E_b, must at that point be approximately equal to k_bT (k_b is Boltzmann's constant and T is temperature), we find E_b to be on the order of several meV.

The characteristic frequency of the RTS f_c is assumed to depend exponentially on the energy barrier to ionic motion. The barrier energy depends on the specific ionic configuration. Furthermore, the application of a voltage across the junction will affect the barrier height differently depending on the overall arrangement relative to the potential gradient. Thus it is not surprising that the frequency f_c of the switching may go up or down with voltage.

The conductance fluctuation, $\partial G/G$, associated with a single RTS should be proportional to the area affected by the switching event divided by the total junction area. The area affected by the trapping of a carrier and the related ionic reconfiguration is, in our model, determined by the smaller of either the dielectric screening length or the size of the defected YBCO region. The length scale estimated from the measured conductance fluctuations is about 170 Å, which is not an unreasonable number for either the screening length in defected YBCO, or the size of those defected regions.

In summary, YBCO/CRO edge junctions exhibit low, $1/f$ noise in the range of operating temperatures from 65 to 77 K. At lower temperatures the level of $1/f$ noise increases, and additionally, telegraph noise dominates the noise power spectrum at discrete, junction-dependent current biases. The characteristic frequency of a particular switching process increases with temperature but may increase or decrease with increased bias current. It is believed that the telegraph noise reflects individual carrier trapping sites at the superconductor-normal metal interface due to oxygen deficiencies and/or disorder.

We would like to thank Chuck Rogers for critically reviewing this manuscript and John Rowell for helpful discussions on the work and ideas presented.

[1] K. Char, M. S. Colclough, T. H. Geballe, and K. E. Myers, Appl. Phys. Lett. **62**, 196 (1993).
[2] K. Char, L. Antognazza, and T. H. Geballe, Appl. Phys. Lett. **63**, 2420 (1993).
[3] M. Matsuda and S. Kuriki, Appl. Phys. Lett. **53**, 621 (1988).
[4] M. Kawasaki, P. Chaudari, and A. Gupta, Phys. Rev. Lett. **68**, 1065 (1992).
[5] A. H. Miklich, John Clarke, M. S. Colclough, and K. Char, Appl. Phys. Lett. **60**, 1899 (1992).
[6] G. Friedl, V. Vildi'c, B. Roas, D. Uhl, F. Bömmel, M. Römheld, B. Hillenbrand, B. Stritzker, and G. Daalmans, Appl. Phys. Lett. **60**, 3048 (1992).
[7] H. K. Olsson, P-Å. Nilsson, Z. Ivanov, R. H. Koch, E. A. Stepantsov, and A. Ya. Tzalenchuk, Appl. Phys. Lett. **61**, 861 (1992).
[8] A. H. Cardona, H. Suzuki, T. Yamashita, K. H. Young, and L. C. Bourne, Appl. Phys. Lett. **62**, 411 (1993).
[9] One exception was the early work by Matsuda and Kuriki in which the noise was found to have a power spectrum dominated by a small number of individual Lorentzian peaks.
[10] C. T. Rogers and R. A. Buhrman, Phys. Rev. Lett. **53**, 1272 (1984).
[11] B. H. Moeckly, D. K. Lathrop, and R. A. Buhrman, Phys. Rev. B **47**, 400 (1993).
[12] C. T. Rogers and R. A. Buhrman, IEEE Trans. Magn. **19**, 453 (1983); C. T. Rogers and R. A. Buhrman, Phys. Rev. Lett. **55**, 859 (1985).

Properties of $YBa_2Cu_3O_{7-x}/YBa_2Cu_{2.79}Co_{0.21}O_{7-x}/YBa_2Cu_3O_{7-x}$ edge junctions

K. Char, L. Antognazza, and T. H. Geballe
Conductus, Inc., Suunyvale, California 94086

(Received 16 May 1994; accepted for publication 16 June 1994)

We report the properties of $YBa_2Cu_3O_{7-x}/YBa_2Cu_{2.79}Co_{0.21}O_{7-x}/YBa_2Cu_3O_{7-x}$ junctions in an edge junction geometry as a function of temperature and barrier thickness. The barrier material used in this work, $YBa_2Cu_{2.79}Co_{0.21}O_{7-x}$, is an underdoped version of $YBa_2Cu_3O_{7-x}$, which has a lower carrier density, a lower T_c, and a higher anisotropy than $YBa_2Cu_3O_{7-x}$. The resistances of the junctions are proportional to the thicknesses of their barriers, suggesting the presence of very little interface resistance. The temperature dependences of critical currents and junction resistances show behavior consistent with that predicted by the conventional proximity effect.

In our recent study[1] we investigated the interface resistances between $YBa_2Cu_3O_{7-x}$(YBCO) and various barrier materials in the epitaxial edge junction geometry. In the case of pseudocubic (CaSr)RuO_3 and $La_{0.5}Sr_{0.5}CoO_3$ barriers we have attributed interface resistances of 10^{-8}–10^{-7} Ω cm^2 to oxygen defects at the YBCO interface, as distinct from the resistance of the barrier itself. The magnitude and the temperature dependence of the interface resistance have been found to be close to that found in high angle grain boundaries,[2] and in YBCO/Au or Ag/YBCO junctions[3] as well. In contrast, when the barrier materials are made of layered structures such as $(LaSr)_2CuO_4$, $YBa_2Cu_{2.79}Co_{0.21}O_{7-x}$(Co-YBCO), and $Y_{0.7}Ca_{0.3}Ba_2Cu_3O_{7-x}$, the interface resistances have been found to be smaller than 10^{-10} Ω cm^2. In this letter, we report the properties of YBCO/Co-YBCO/YBCO junctions in detail as functions of temperature and thickness. We show that the temperature dependences of critical currents and junction resistances are quantitatively and qualitatively different from those of junctions with 10^{-8}–10^{-7} Ω cm^2 interface resistances.

Co-YBCO is an underdoped version of YBCO; the carrier density and the critical temperature are reduced and the anisotropy is increased. It has been found that Co atoms go to the Cu site in the Cu-O chain layer, grab extra oxygen, and distort the lattice slightly.[4] It is believed that the Co-O environment reduces the number of holes in the system, in much the same way that oxygen deficiency in the Cu-O chain layer does. There are other atoms such as Al, Ga, and Fe which are known to substitute for Cu sites in the Cu-O chain layer and they behave in a similar way to Co. There are two other ways to dope and reduce T_c in the YBCO system. One way is to increase the carrier density and drive YBCO into the overdoped region. Ca-doped YBCO[5] is an example of overdoped YBCO. Overdoped high T_c materials are known to have higher carrier density, lower T_c, and smaller anisotropy than YBCO. The properties of junctions using Ca-doped YBCO are described in a separate letter.[6] The other way is to modify the Cu-O_2 plane layers by doping with Pr, Ni, and Zn. when Pr, Ni, and Zn replace both Y in the plane adjacent to the Cu-O_2 plane and also Cu in the Cu-O_2 plane layer, these dopants eventually modify the double Cu-O_2 plane layers, lowering the critical temperature. In the case of Ni and Zn doping, the mechanism for the lower critical temperature is believed to be increased scattering of the carriers, as suggested by the temperature dependence of the resistivities and the Hall coefficients. In the case of Pr, both reduced carrier concentration and increased scattering seem likely. We believe that Co-doped barriers are the most likely to approach ideal junction behavior, and therefore have concentrated our efforts on them.

Figure 1 shows the temperature dependence of an epitaxial Co-YBCO film deposited by laser ablation on a $LaAlO_3$ substrate. The resistivity of 1 $\mu\Omega$ cm at 300 K linearly decreases as the temperature decreases and the film goes through a superconducting transition around 50 K. The magnitude and temperature dependence of the Co-YBCO film resistivity agree very well with results for single crystals.[7] The fact that the resistivity still extrapolates to zero value at zero temperature suggests that the increase in resistivity is due to reduction in carrier density rather than increased scattering. This temperature dependence of resistivity is almost identical to that of an oxygen-deficient YBCO single crystal reported recently.[8]

The description of our edge junction fabrication process

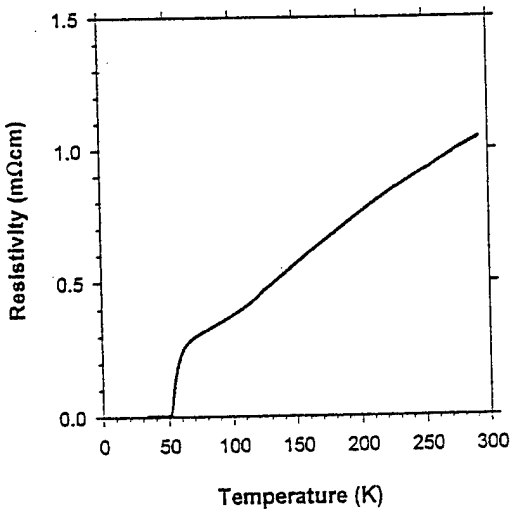

FIG. 1. Resistivity vs temperature for a 100-nm-thick epitaxial Co-YBCO film.

 0003-6951/94/65(7)/904/3/$6.00

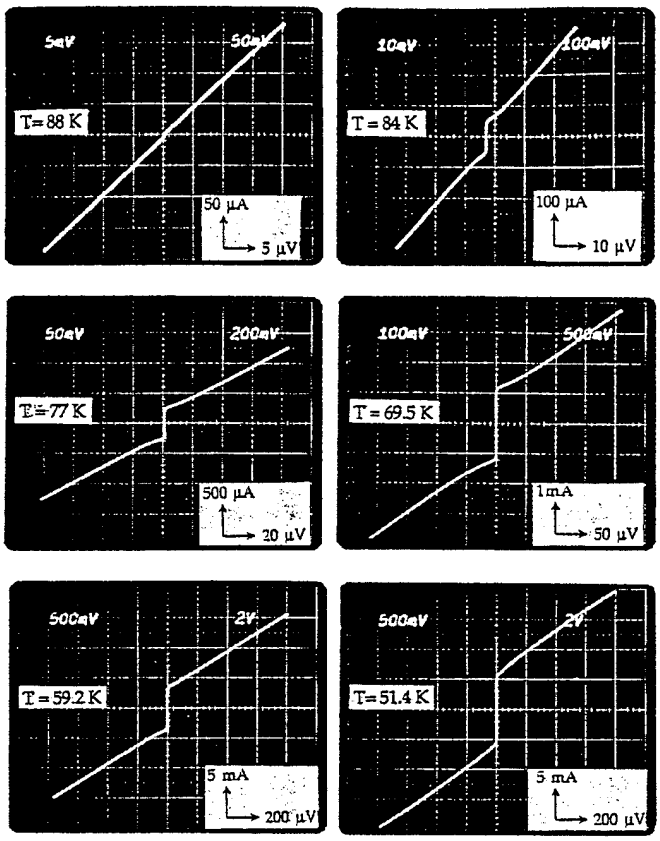

FIG. 2. I-V characteristics of a junction with a 150 Å Co-YBCO barrier at several temperatures.

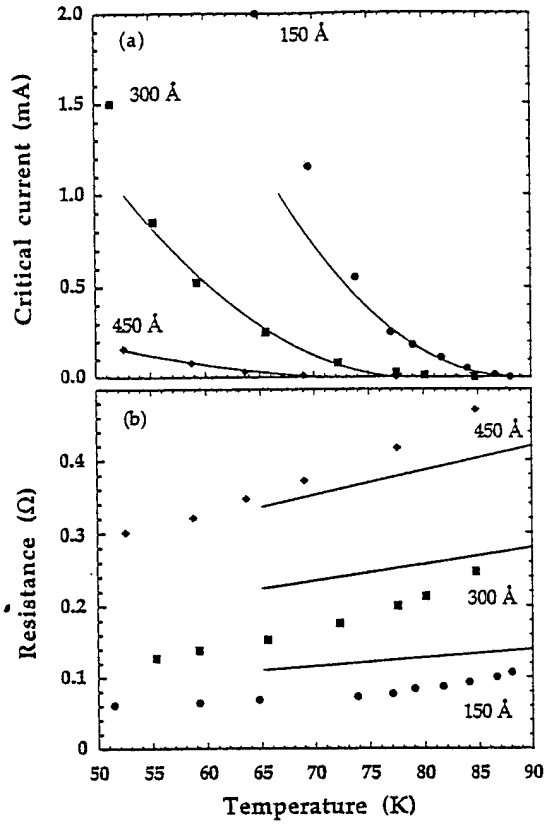

FIG. 3. (a) Temperature dependence of critical currents and (b) temperature dependence of junction resistances at various Co-YBCO barrier thicknesses. The solid lines in (a) are fits to $(T-T_c)^2$ dependence. The solid lines in (b) represents the temperature dependence of the bulk film resistivity scaled for each barrier thickness. Each calculated resistance has been multiplied by 1.5 to better fit the data of the three barrier thicknesses.

is given in other publications.[1,9] Briefly describing the process, we use a c-axis oriented edge junction geometry to take advantage of transport in the Cu-O_2 planes as well as small junction areas. First, the YBCO layer and $SrTiO_3$ insulating layer are deposited and this bilayer is patterned by Ar ion beam milling. This milling produces a slope of YBCO with an angle of about 30° to the substrate. Second, the Co-YBCO barrier layer and YBCO counterelectrode layer are deposited and patterned. Au contacts are deposited on the first and second YBCO pads to provide low noise contacts. It is worth making two points before we describe the behavior of the junctions. First YBCO/YBCO contacts made in an edge junction structure without any barrier layer carried a critical current density higher than 1×10^6 A/cm^2. This suggests that the ion-mill-damaged YBCO surface is restored during the heating for the second barrier/YBCO deposition. This was recently confirmed[10] by transmission electron microscopy. Second, when we used a 10-nm-thick $SrTiO_3$ layer as the barrier layer in several junctions, they did not show any zero voltage current, even though the resistance of the junctions varied between tens of ohms and hundreds of kilo-ohms.

Figure 2 displays the current-voltage characteristics (I-V) of a junction with a 150-Å-thick Co-YBCO barrier layer at several temperatures. As soon as both YBCO electrodes become superconducting, a resistance of about 0.1 Ω is measured around 88 K. This value corresponds well with the expected bulk resistance of the barrier, which is about 350 $\mu\Omega$ cm$\times$150 Å/(4 μm$\times$0.15 μm)=0.09 Ω. As the temperature decreases, the critical current, I_c, increases and the resistance, R_n slightly decreases. The I-V characteristics fit closely with a resistively shunted junction (RSJ) model. When I_c starts to exceed about 1 mA, an excess current starts to develop, meaning that the high bias resistance no longer extrapolates to zero current at zero voltage. We believe that this is a crossover to a long junction behavior when the width of the junction becomes larger than the Josephson penetration depth.[11] As the critical current goes about 5 mA, the I-V characteristics show flux–flow-like bending around 51 K. However, at the same temperature, in the case of junctions with thicker Co-YBCO barrier, the I-V characteristics remain like a RSJ, suggesting that the crossover to a flux-flow-like behavior is determined by the magnitude of the critical current (i.e., the strength of coupling) rather than the temperature being close to the critical temperature of the barrier.

The temperature dependences of I_c and R_n of junctions with YBCCoO barrier thicknesses of 150, 300, and 450 Å are shown in Fig. 3. The temperature dependence of I_c in Fig. 3(a) can be well described by $I_c(T)=I_{c0}(T-T_c)^2$, as expected from conventional SNS theory.[12] The reduction of the T_c of the junctions with the thickness of the barrier is also consistent with the conventional proximity effect. On

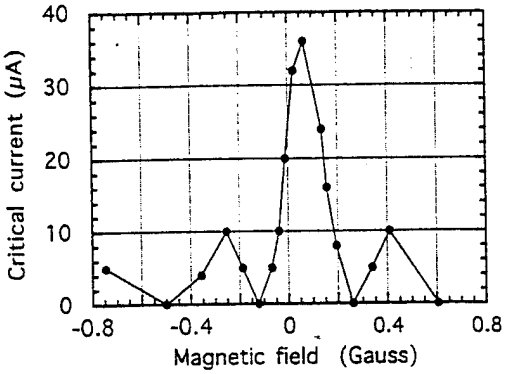

FIG. 4. Magnetic field modulation of the critical current of a junction with a 300 Å Co-YBCO barrier at 77 K.

the other hand, the temperature dependences of R_n of the junctions generally follow that of the bulk barrier material, as shown in Fig. 1. The fact that the junction resistances scale well with the thicknesses of the barrier suggests that the interface resistances are much smaller than the bulk resistance of the barrier. However, when I_c is high, so that the I-V characteristics of the junctions are not like RSJ, the measured junction resistances drop faster than the bulk value of the barrier. This effect is more pronounced in the case of Ca-doped YBCO barrier junctions.[6] In low T_c superconductors,[13] this was understood in terms of the development of a pair potential, Δ_n, in the barrier due to its own pair interaction potential (the barrier itself is a superconductor), eventually making Andreev reflection take place inside the barrier instead of at the SN interface. It is known that Andreev reflection takes place in the case of a clean boundary, consistent with scaling of the junction resistance with the thickness of the barrier.

From Fig. 3(a) we can estimate the normal coherence length of the Co-YBCO barrier around 70 K, since all three junctions with the different thicknesses maintain RSJ characteristics at that temperature. Assuming an exponential decay of critical current as a function of thickness, the normal coherence length of Co-YBCO can be estimated to be around 70 Å. On the other hand, if we calculate the normal coherence length $\xi_n = v_F \hbar / 2\pi k_B T$ in the clean limit with $v_F = 3\times10^7$ cm/s, ξ_n comes out to be 54 Å at 70 K. Given the uncertainty of the edge junction geometry, the measured value seems to agree well with the calculated value.

The magnetic field diffraction pattern of I_c of a junction with a barrier thickness of about 200 Å at 77 K is shown in Fig. 4. This particular thickness of barrier is chosen for the I_c value to be smaller than 100 μA at 77 K, since the modulation usually is not complete when I_c is higher than 100 μA. The magnetic field was perpendicular to the substrate, and the effective junction area came out to be about 40 μm^2. This is much larger than the real geometry of the junction and is due to the flux focusing effect in planar type junctions, especially from the wide first YBCO layer. We still do not completely understand the effect of edge angle, anisotropy of the YBCO and the barrier, shielding from the upper YBCO electrode as well as flux focusing on the behavior of the junction in a magnetic field.

It is possible that Co atoms are diffusing in the barrier region. In order to investigate this possibility, we made superlattices of 24 Å YBCO and 24 Å 7% Co-doped YBCO. The critical temperature of the superlattice was found to be 81 K, which is higher than the T_c of 3.5% Co-doped YBCO, suggesting the diffusion of Co in the c-direction is not significant over the length scale of two unit cells. However, the diffusion may be higher in the a and b directions and this will need further study, which is underway using transmission electron microscopy.

In summary, we have reported detailed values of I_c and R_n as a function of temperature and barrier thickness in epitaxial SNS edge junctions with 7% Co-doped YBCO barriers. A normal coherence length of about 70 Å at 70 K and very little interface resistance have been measured. These junctions are qualitatively and quantitatively different from numerous other junctions with 10^{-8}–10^{-7} Ω cm^2 interface resistances. We believe that the behavior of these junctions is closer to that expected from the conventional proximity effect.

We would like to thank Laura King and Art Sleight at Oregon State University for providing the initial Co-doped YBCO material. We would like to thank Elena Corpuz for her technical support and appreciate discussions with John Rowell, Randy Simon, and John Clarke. This work has been supported by Naval Research Laboratory Grant No. N00014-93-C-2054 and Air Force SBIR Grant No. F49620-93-C-0058.

[1] K. Char, L. Antognazza, and T. H. Geballe, Appl. Phys. Lett. **63**, 2420 (1993).
[2] K. Char, M. S. Colclough, L. P. Lee, and G. Zaharchuk, Appl. Phys. Lett. **59**, 2177 (1991).
[3] M. S. DiIorio, S. Yoshizumi, K.-Y. Yang, J. Zhang, and M. Maung, Appl. Phys. Lett. **58**, 2552 (1991); R. H. Ono, J. A. Beall, M. W. Cromar, T. E. Harvey, M. E. Johansson, C. D. Reintsema, and D. A. Rudman, *ibid.* **59**, 1126 (1991).
[4] G. G. Li, F. Bridges, J. B. Boyce, and W. C. H. Joiner, Phys. Rev. B **47**, 12110 (1993); R. S. Howland, T. H. Geballe, S. S. Laderman, A. Fisher-Colbrie, M. Scott, J. M. Tarascon, and P. Barboux, Phys. Rev. B **39**, 9017 (1989).
[5] Y. Tokura, J. B. Torrance, T. C. Huang, and A. I. Nazzal, Phys. Rev. B **38**, 7156 (1988); H. M. Appelboom, H. Sato, and M. Naito, Physica C **221**, 125 (1994).
[6] L. Antognazza, K. Char, and T. H. Geballe, Appl. Phys. Lett. (submitted).
[7] A. Carrington, A. P. Mackenzie, C. T. Lin, and J. R. Cooper, Phys. Rev. Lett. **69**, 2855 (1992).
[8] T. Ito, K. Takenaka, and S. Uchida, Phys. Rev. Lett. **70**, 3995 (1993).
[9] K. Char, M. S. Colclough, T. H. Geballe, and K. E. Myers, Appl. Phys. Lett. **62**, 196 (1993).
[10] E. Olsson and K. Char, Appl. Phys.Lett. **64**, 1292 (1994).
[11] T. Van Duzer and C. W. Turner, *Principles of Superconductive Devices and Circuits* (Elsevier, New York, 1981), Chap. 4.
[12] See, for instance, P. G. DeGennes, *Superconductivity of Metals and Alloys* (Benjamin, New York, 1966).
[13] J. Clarke, S. M. Freake, M. L. Rappaport, and T. L. Thorp, Solid State Commun. **11**, 689 (1972).

Proximity effect in $YBa_2Cu_3O_{7-\delta}/YBa_2(Cu_{1-x}Co_x)_3O_{7-\delta}/YBa_2Cu_3O_{7-\delta}$ junctions: From the clean limit to the dirty limit with pair breaking

L. Antognazza, S. J. Berkowitz, T. H. Geballe,* and K. Char
Conductus, Inc., Sunnyvale, California 94086
(Received 3 October 1994)

We report on the proximity effect observed in $YBa_2Cu_3O_{7-\delta}/YBa_2(Cu_{1-x}Co_x)_3O_{7-\delta}/YBa_2Cu_3O_{7-\delta}$ junctions in an edge-junction geometry where $x=0.04$, 0.07, and 0.14. The temperature, thickness, and doping dependence of the critical current of the junctions can be well described by the proximity-effect theory, due to very little interface resistance. We observed a crossover from the clean limit to the dirty limit behavior where a pair-breaking scattering time $\tau_{pb}=6\times10^{-14}$ sec, consistent with short-range magnetic fluctuations in the barrier, was found.

We report a systematic study of superconductor-normal-superconductor (SNS) Josephson behavior involving the high-T_c cuprates. The junctions are found to crossover from the clean limit to the dirty limit where a new pair-breaking scattering appears. The SNS behavior is determined by the proximity effect and this depends upon behavior of Josephson pairs which leak into the barrier material which in turn provides information regarding the interaction potential in the barrier material. Different scattering mechanisms such as elastic scattering which maintains the pairing phase coherence, and inelastic or magnetic scattering which destroys it, can be studied through the proximity effect. In this paper we report the Josephson properties of high-T_c SNS junctions which can be analyzed within the framework of the same de Gennes' proximity theory[1] used for conventional superconductors. Our barrier layers are Co-doped YBCO, whose doping level can be easily controlled, since the interface between YBCO and Co-doped YBCO has been shown to be very clean.[2,3]

In the Josephson junctions which have been used recently[4–6] in important investigations of the wave-function symmetry of $YBa_2Cu_3O_{7-\delta}$ (YBCO), an ambiguity which has not been explicitly addressed is the excess resistance. The origin of the excess resistance is believed to be due to degraded YBCO as result of oxygen deficiency and disorder adjacent to the interface. In order to clarify the exact transport mechanism through such ill-defined YBCO interfaces, it is desirable to investigate Josephson coupling through interfaces that are well defined and can be controlled, as in the present study. Previous studies have been with elements such as Ag and Au,[7] as well as $PrBa_2Cu_3O_{7-\delta}$,[8] $Y_{0.6}Pr_{0.4}Ba_2Cu_3O_{7-\delta}$,[9] $CaRuO_3$,[10] and $SrRuO_3$,[11] all of which, when measured, have had significant interface resistances on the order of 10^{-8}–10^{-7} Ωcm^2. The SNS junctions reported here have two or more orders of magnitude less interface resistance.

Our recent study of edge junctions[3] indicates the mismatch of thermal-expansion coefficients at the interface is an important factor in the excess interface resistance. A matching coefficient of expansion in the c direction can be achieved by using a related metallic layered structure. $PrBa_2Cu_3O_{7-\delta}$ (Ref. 8) and Pr-doped YBCO (Ref. 9) are, of course, such examples. These materials, unfortunately, have other types of disorder that result in barriers that are difficult to quantify. The Pr is believed to hybridize[12] with the oxygen in the CuO_2 planes thus removing carriers but leaving localized states on or adjacent to the CuO_2 planes. The residual transport in the CuO_2 planes of undoped $PrBa_2Cu_3O_{7-\delta}$ is by variable range hopping, an inelastic process which destroys phase coherence. The long-range proximity which is sometimes observed may involve the CuO chains and be very sensitive to small changes in oxygen concentration.[13] The use of Y to dope the barriers into the metallic degraded superconducting state $(Pr_{1-x}Y_x)Ba_2Cu_3O_{7-\delta}$ introduces an intrinsic disorder in the CuO_2 planes.

There are three other strategies for obtaining barriers with the favorable structural and coefficient of expansion features. One is to increase the carrier density and drive YBCO into the overdoped region; Ca-doped YBCO is an example of such overdoped YBCO. The proximity effect using Ca-doped YBCO will be described in a separate paper.[14] A second is to reduce the carrier concentration by cation substitution on lattice sites remote from the CuO_2 planes and thus minimize the introduction of disorder on the CuO_2 planes. This is the strategy employed here. A third way to dope YBCO and lower its T_c is to replace Cu atoms directly on the Cu-O_2 plane layers using, for example, Zn or Ni. It is known[15] that the increased scattering decreases T_c even through the carrier density remains basically the same.

Figure 1 shows the temperature dependence of an 1000-Å-thick epitaxial $YBa_2(Cu_{1-x}Co_x)_3O_{7-\delta}$ (Co-doped YBCO) film on a $LaAlO_3$ substrate deposited by laser ablation. At the low doping level of 4% ($x=0.04$) and 7% ($x=0.07$), the resistivity still extrapolates to near zero value at zero temperature with a slight curvature, suggesting that the increase in resistivity is due to reduction in carrier density rather than increased scattering. This temperature dependence of resistivity is almost identical to that found in Co-doped YBCO single crystals[16] and in oxygen-deficient YBCO single crystals.[17] For the highest

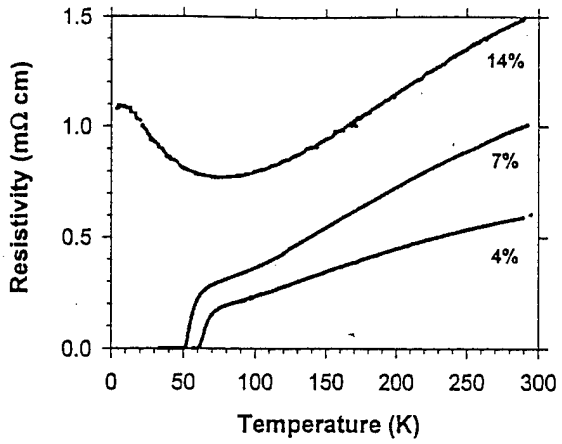

FIG. 1. Resistivity vs temperature curve of three epitaxial Co-doped YBCO films.

doping level of 14%, the high-temperature linear resistivity no longer extrapolates to zero value at zero temperature. For a given composition there is some dependence of T_c and the temperature dependence of the resistivity on the film-growth condition. We have chosen to work with the deposition conditions that generate the best x-ray-diffraction pattern, which also generate the highest resistivity slope for a given nominal composition.

Our junction process is described in detail elsewhere.[10] The thickness of both YBCO layers was between 1500 and 2000 Å, and the width of the junctions is 4 μm. All the junctions were made on $LaAlO_3$ substrates, and the edges were patterned in the twinned (100) or (010) direction. For each doping level and thickness, we have tested ten junctions on two different substrates. The variation of the critical currents was $\pm 25\%$ and the resistances had variations of $\pm 10\%$. For each doping level and thickness, we have selected a junction whose critical current value is in the middle of the distribution and measured its temperature dependence, as reported in Figs. 2, 3, and 4.

The conventional proximity effect given by de Gennes[1] predicts

$$I_c = I_0(1-t)^2 \frac{\kappa d}{\sinh(\kappa d)} = \frac{18.5\text{mV}}{R_n}(1-t)^2 \frac{\kappa d}{\sinh(\kappa d)} , \quad (1)$$

where $t = T/T_c$, $T_c = 88$ K, $I_0 = \pi\Delta_0^2/4R_n k_B T_c = 18.5$ mV$/R_n$ in the case of BCS gap $2\Delta_0 = 3.52 k_B T_c$, d is the thickness of the barrier, and κ^{-1} is the decay length. Even though this relation was derived in the dirty limit near T_c, the thickness, temperature and doping dependence of our data can be surprisingly well described by Eq. (1) with very reasonable microscopic parameters. Since the electronic mismatch between YBCO and Co-doped YBCO is not significant, we used $(1-t)^2$ dependence, assuming continuous boundary conditions of the wave function and its derivative.[1]

The temperature dependence of the critical current and the resistance of 14% Co-doped junctions are shown in Fig. 2 for three different nominal thicknesses of 150, 300, and 450 Å. From the simple exponential relation between the critical current and the thickness of the barrier, $I_c \propto \exp(-\kappa d)$, the decay length κ^{-1} is plotted at several temperatures in the inset of Fig. 2. In order to find out whether the 14% Co-doped YBCO junctions are in the clean limit or in the dirty limit, $\kappa^{-1}(T)$ has been fitted with T^{-1} and $T^{-1/2}$ temperature dependences, since $\kappa^{-1} = v_F\hbar/2\pi k_B T$ in the clean limit and $\kappa^{-1} = (D\hbar/2\pi k_B T)^{1/2}$ in the dirty limit. Here v_F is the Fermi velocity and D is the diffusion constant. It is clear the 14% Co-doped YBCO is in the dirty limit as shown in the inset of Fig. 2.

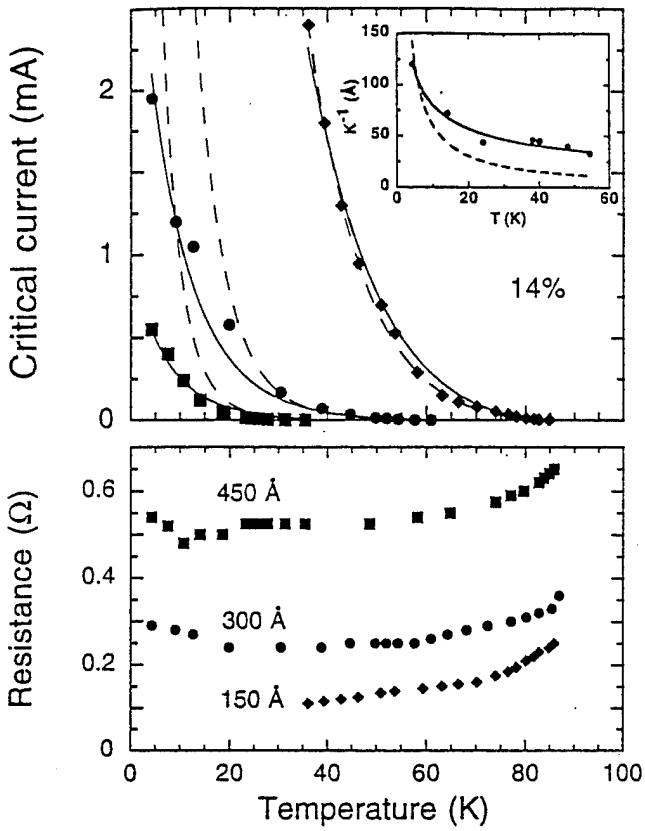

FIG. 2. Temperature dependence of critical currents and resistances of 14% Co-doped YBCO junctions with barrier thickness of 150, 300, and 450 Å. The solid lines are fits to Eq. (1) with a pair-breaking scattering rate of $\tau_{pb} = 6\times10^{-14}$ sec. The dotted lines are fits to Eq. (1) without a pair-breaking scattering. The inset shows the decay length κ^{-1} as a function of temperature for 14% Co-doped YBCO junctions. The solid line is a fit to $T^{-1/2}$ dependence and the dotted line is a fit to T^{-1} dependence.

In the dirty limit when the barrier material is superconducting with its transition at T_n, the decay length is expressed by

$$\kappa^{-1} = \left[D\frac{\hbar}{2\pi k_B T}\right]^{1/2}\left[1+\frac{2}{\ln(T/T_n)}\right]^{1/2} , \quad (2)$$

where the diffusion constant $D = v_F 1/3$. Using $T_n = 0$, and the measured R_n right below T_c,[18] the I_c values in Fig. 2 have been fitted with L being the only parameter where the dimensionless L is defined by $\kappa d = L(T/T_c)^{1/2}$. The dotted lines are such fits with $L = 7.2$, 13, and 16.5, which yields the average diffusion constant $D = 4.1$ cm^2/sec. The scaling of L with the nominal bar-

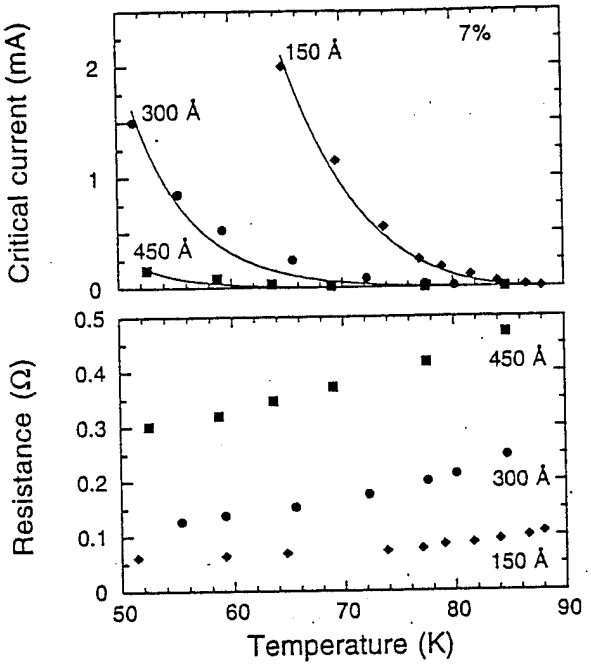

FIG. 3. Temperature dependence of critical currents and resistances of 7% Co-doped YBCO junctions with barrier thickness of 150, 300, and 450 Å. The solid lines are fits to a dirty limit and the overlapping dotted lines are fits to a clean limit.

rier thickness[19] or with the measured resistances is not very good and the fits are poor especially at low temperature. The problem is that the critical currents do not increase as fast as the Eq. (1) predicts at low temperatures, suggesting a cutoff scattering rate of superconducting pairs. This behavior has been observed in low-T_c system[20] when the barrier material has magnetic impurities which destroys superconducting pairs.

When there is a pair-breaking scattering in the barrier material, the lifetime of superconducting pairs inside the barrier is modified. The effective lifetime will be given[21] by

$$\frac{1}{\tau_{\text{eff}}}=\frac{1}{\tau}+\frac{1}{\tau_{\text{pb}}}=\frac{2\pi k_B T}{\hbar}+\frac{2\pi k_B T_{\text{pb}}}{\hbar}=\frac{2\pi k_B (T+T_{\text{pb}})}{\hbar}. \tag{3}$$

The net effect is that T is replaced by $T+T_{\text{pb}}$ in Eq. (2). The fitting to this new temperature with $T_{\text{pb}}=20$ K is shown as solid lines in Fig. 2, with $L=5.9$, 10.5, and 12.2, which yields the diffusion constant $D=6.6$ cm^2/sec with a better scaling with the nominal thickness and with the measured resistances. The data are fit nicely in the 14% Co-doped barrier with a pair-breaking scattering time $\tau_{\text{pb}}=\hbar/2\pi k_B T_{\text{pb}}=6\times10^{-14}$ sec. Since the junctions are well described by the dirty-limit formula, it also suggests that superconducting pairs still experience more weak elastic scattering than pair breaking. This is consistent with the fact that the resistivity of the barrier does not extrapolate to zero at zero temperature as shown in Fig. 1. The origins of the pair-breaking scattering is not obvious. It could simply be that the 42% (three times 14%) doping on the chains induces enough disorder to cause pair breaking by strong elastic scattering. Alternatively, the spin-glass state of underdoped nonsuperconducting YBCO can result in magnetic pair breaking on the CuO_2 planes. We rule out the possibility that segregated cobalt oxide may cause the pair breaking, since x-ray-absorption fine structure[22] (XAFS) on Co-doped YBCO did not show evidence of cobalt oxide segregation. We also point out that the slowdown of the critical current at low temperature is not due to the critical current saturation observed for large junctions of in-line geometries, since the critical current saturation is not expected for the overlap geometry[23] of our edge junctions. This is further confirmed by the good fit up to the 2.5-mA current level for the 150-Å-thick barrier junction and also by the fact that the 450-Å-thick barrier junction is not even in the large junction limit as its critical current is small.

The temperature dependence of critical currents and resistances of the 7 and 4% Co-doped YBCO junctions are shown in Figs. 3 and 4, respectively. Initially, we analyzed the data in terms of dirty-limit formulas given by Eq. (2). The fits are shown in the figures as solid lines. For the 7% doping, $T_n=40$ K was used[24] for the fitting and L was found to be 10, 16.5, and 23 where

$$\kappa d=L\left[\frac{T}{T_c}\right]^{1/2}\left[1+\frac{2}{\ln(T/T_n)}\right]^{-1/2}$$

For the 4% doping, L was found to be 12, 17.2, and 22.5 with $T_n=55$ K.[24] From the fits the average diffusion constants were found to be $D=2.2$ cm^2/sec for 7% and $D=2$ cm^2/sec for 4%. These values are unphysical when compared to $D=6.6$ cm^2/sec found for 14% Co-doped barrier, since the diffusion constant should increase as the doping level decreases, according to $D=v_F l/3$. This

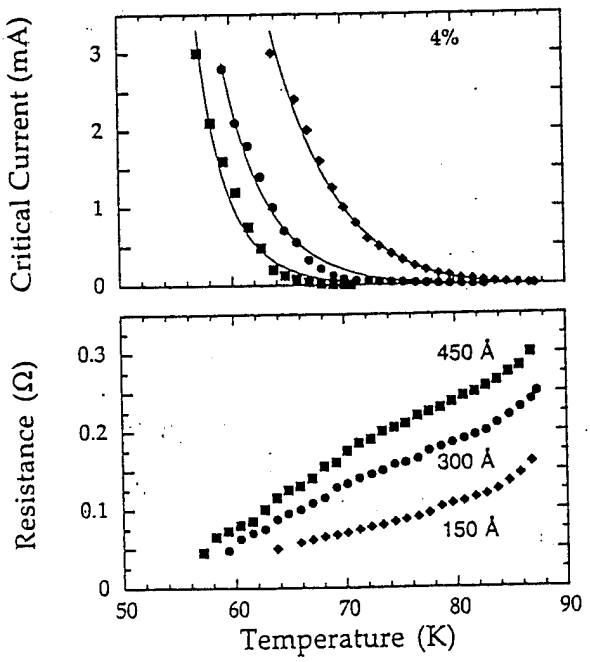

FIG. 4. Temperature dependence of critical currents and resistances of 4% Co-doped YBCO junctions with barrier thickness of 150, 300, and 450 Å. The solid lines are fits to a dirty limit and the overlapping dotted lines are fits to a clean limit.

suggests that the decay length of 7 and 4% Co-doped material is not determined by the diffusion constant, and thus that these materials are in the clean limit.

In the clean limit, according to the Ginzburg Landau theory, the decay length of a superconductor above its critical temperature T_n is given by[9] $\kappa^{-1}=\sqrt{2}\times 0.74\xi_0(T/T_n-1)^{-1/2}$, where the BCS coherence is given by $\xi_0=\hbar v_F/\pi\Delta$. The fits to this relation are shown as the dotted lines in Figs. 3 and 4. For 7% doping, L was found to be 4.8, 7.9, and 11 where $\kappa d=L(T/T_n-1)^{1/2}$ and $T_n=40$ K was used. In case of 4% doping, L was found to be 6.7, 9.6, and 12.6 with $T_n=55$ K. The fits are overlapping with the solid lines given by the dirty-limit formula. This is not surprising since it is easy to show that the Eq. (2) can be modified to $\kappa^{-1}\propto(T/T_n-1)^{-1/2}$ when T is near T_n, where even the dirty-limit formula is supposed to follow the Ginzburg-Landau relation. However, the average BCS coherence lengths we obtain from the fitting with the clean limits, 35 Å for 7% Co-doped YBCO and 28 Å for 4% Co-doped YBCO, are consistent with the BCS formula $\xi_0=\hbar v_F/\pi\Delta$. The small increase with doping follows from Fermi velocity, not decreasing as much as the critical temperature when the doping increases. We take the above analysis as strong evidence that the 4 and 7% Co-doped YBCO are indeed in the clean limit.

YBCO itself is known[25] to be in the clean limit. As the Co doping increases, the carrier density and the critical temperature decrease, increasing the BCS coherence length according to $\xi_0=\hbar v_F/\pi\Delta$, as long as Co-doped YBCO remains in the clean limit. As the doping level is further increased beyond 7%, the decreasing mean free path eventually becomes smaller than the increasing clean-limit coherence length, causing a crossover to the dirty limit. In this regime the coherence length decreases with increased doping and both elastic scattering and pair-breaking scattering are required to fit the data.

We would like to thank Elena Corpuz for her technical support and we appreciate the very useful discussions with John Clarke and John Rowell. This work has been supported by Naval Research Laboratory Grant No. N00014-93-C-2054 and Air Force SBIR Grant No. F49620-93-C-0058.

---

*Also at the Dept. of Applied Physics, Stanford University, Stanford, CA 94305.

[1]P. G. De Gennes, Rev. Mod. Phys. **36**, 225 (1964).

[2]K. Char *et al.*, Appl. Phys. Lett. **65**, 904 (1994).

[3]K. Char *et al.*, Appl. Phys. Lett. **63**, 2420 (1993).

[4]D. A. Wollman *et al.*, Phys. Rev. Lett. **72**, 2134 (1993).

[5]P. Chaudhari and Shawn-Yu Lin, Phys. Rev. Lett. **72**, 1084 (1994).

[6]A. G. Sun *et al.*, Phys. Rev. Lett. **72**, 2267 (1994).

[7]M. S. DiIorio *et al.*, Appl. Phys. Lett. **58**, 2552 (1991); R. H. Ono *et al.*, *ibid.* **59**, 1126 (1991).

[8]J. B. Barner *et al.*, Appl. Phys. Lett. **59**, 1629 (1991); T. Hashimoto *et al.*, *ibid.* **60**, 1756 (1992).

[9]E. Polturak *et al.*, Phys. Rev. Lett. **67**, 3038 (1991).

[10]K. Char *et al.*, Appl. Phys. Lett. **62**, 196 (1993).

[11]L. Antognazza *et al.*, Appl. Phys. Lett. **63**, 1005 (1993).

[12]R. Fehrenbacher and T. M. Rice, Phys. Rev. Lett. **70**, 1700 (1993).

[13]Y. Suzuki *et al.*, Phys. Rev. Lett. **73**, 328 (1994).

[14]L. Antognazza *et al.* (unpublished).

[15]T. R. Chien *et al.*, Phys. Rev. Lett. **67**, 2088 (1991).

[16]A. Carrington *et al.* Phys. Rev. Lett. **69**, 2855 (1992).

[17]T. Ito *et al.*, Phys. Rev. Lett. **70**, 3995 (1993).

[18]We have used temperature-independent resistance throughout the paper, since the origin of the temperature-dependent resistance especially for low doping case is not clear at this time. If it is due to Andreev reflection or flux motion of Josephson or Abrikosov vortices in or near the junction, the temperature dependence of the junction resistance may not necessarily be that of bulk barrier resistance.

[19]The nominal thickness is based on deposition time. However, the deposition rate in laser ablation is known to change in time and there is a slight change in deposition rate run to run.

[20]J. L. Patterson, J. Low Temp. Phys. **35**, 371 (1979).

[21]G. Deutscher and P. G. de Gennes, *Superconductivity,* edited by R. D. Parks (Marcel Dekker, New York, 1969), Chap. 17.

[22]G. G. Li *et al.*, Phys. Rev. B **47**, 12 110 (1993).

[23]Antonio Barone and Gianfranco Paternó, *Physics and Applications of the Josephson Effect* (Wiley, New York, 1982), Sec. 5.3.

[24]T_n was found lower than the superconducting transition temperature of a 1000-Å-thick bulk film measured without patterning. It is not unreasonable to assume that thinner films grown on the edges of YBCO patterned into a 4-μm-wide bridge may have a lower T_n, especially given the fact that T_n can change as much as 10 K even in a bulk film depending on the deposition conditions. A slightly different value may be used with reasonable fits to data. However the change in D value due to different T_n value does not affect the systematic conclusions we have found.

[25]See, for example, K. Kamáras *et al.*, Phys. Rev. Lett. **64**, 84 (1990).